Carbon Letters (2022) 32:339–364
https://doi.org/10.1007/s42823-021-00276-9

Online ISSN 2233-4998
Print ISSN 1976-4251

REVIEW

A review of gas sensors based on carbon nanomaterial

Indah Raya[1] · Hamzah H. Kzar[2] · Zaid Hameed Mahmoud[3] · Alim Al Ayub Ahmed[4] · Aygul Z. Ibatova[5] · Ehsan Kianfar[6,7]

Received: 11 July 2021 / Revised: 9 August 2021 / Accepted: 10 August 2021 / Published online: 20 September 2021

Abstract
As a new nanostructure, a graphene is a compound of carbon atoms with a two-dimensional structure that has attracted the attention of many nanoscale researchers due to its novel physical and chemical properties. The presence of all graphene atoms in the surface and its unique electrical properties, as well as the ability to functionalize and combine with another nanomaterial, has introduced graphene as a new and suitable candidate material for gas sensing. Over the years, many researchers have turned their attention to carbon nanomaterial. The unique optical, mechanical, and electronic properties of these nanostructures have led them to use these nanomaterials to develop tiny devices, such as low-consumption sensors. Carbon nanomaterial poses a threat to another nanomaterial in terms of their use in gas sensors. This review article discusses the use of carbon nanoparticles and graphene in gas sensors, examines the nodes in the commercialization pathway of these compounds, and presents the latest achievements. Finally, the perspectives of the challenges and opportunities in the field of sensors based on carbon nanomaterial and graphene are examined.

Keywords Graphene · Nanomaterial · Two-dimensional · Sensors · Carbon nanomaterial · Electronic

1 Introduction

Sensors today are of undeniable importance in industry and research that is can perform detection by quantifying a physical or chemical phenomenon at the sensor surface and converting changes into an electrical, mechanical, or optical signal [1–4]. Today, due to the undeniable applications of gases in industry, agriculture, homes, research, and even outside the atmosphere in the field of space science, detecting and measuring the type and concentration of gases, especially toxic and flammable gases, is inevitable [5–9]. Therefore, the necessity of introducing and manufacturing new sensors from sensitive materials with appropriate selectivity is determined [10, 11]. The field of nanotechnology, with its large number and variety of nanomaterial with high volume, modifiability, and engineering of physical and chemical properties of their surface, introduces many candidates for gas sensing [12]. The dramatic use of nanoparticles, nanowires, and nanotubes as gas sensors and chemical evidence for this claim [13–18]. These new nanostructures, with high effective surface area and improved sensor parameters can be a good alternative to the old sensors, are often based on mineral semiconductors and metal oxides [19, 20]. One of these emerging nanoparticles is graphene as a compound of carbon atoms with hexagonal lattices, which since its discovery in 2004 has attracted the attention of many researchers in various fields—such as Nano electronics, nanophysics, Nano chemistry, nanomaterial, nanoparticles, etc. [21–25]. Placement of all grapheme atoms on the surface, interesting electrical, mechanical and chemical properties, and a variety of manufacturing methods are some of the reasons

✉ Ehsan Kianfar
e-kianfar94@iau-arak.ac.ir; ehsan_kianfar2010@yahoo.com

1 Chemistry Department, Faculty Mathematics and Natural Science, Hasanuddin University, Makassar, South Sulawesi, Indonesia

2 Department of Chemistry, College of Veterinary Medicine, Al-Qasim Green University, Al Qasim, Iraq

3 Chemistry Department, College of Science, Diyala University, Baqubah, Iraq

4 School of Accounting, Jiujiang University, 551 Qianjindonglu, Jiujiang, Jiangxi, China

5 Tyumen Industrial University, Tyumen, Russia

6 Department of Chemical Engineering, Arak Branch, Islamic Azad University, Arak, Iran

7 Young Researchers and Elite Club, Gachsaran Branch, Islamic Azad University, Gachsaran, Iran

that can make graphene a good candidate for sensing [26, 27]. Although graphene itself is a gas-absorbing material, it can achieve better sensitivity and selectivity for gas sensing in hybrid structures with another nanomaterial by taking advantage of the synergistic effect to improve sensitivity and selectivity. one of the limitations of graphene as a gas sensor sensitivity is not so high in the presence of environmental contamination—because of the nature of Lipophilicity, low selectivity, and desorption of the absorbed species problem to return the sensor to initial conditions—he said. Therefore, selecting, designing, and manufacturing new graphene-based hybrid compounds with another nanomaterial is one of the major challenges in this area [28–31]. Over the past few years, the number of articles on nanomaterial gas sensors has increased dramatically. In today's world, electronic sensors strongly need a stable, sensitive, and simple that minimal quantities of gases step, routers choose, it is felt. Such sensors can be used to detect biomass or hazardous chemical agents. At present, the construction of such sensors is costly due to the complexity of materials and equipment, therefore there is a great deal of focus on making cheaper and more efficient sensors [32–35]. Of all the nanomaterial, a carbon nanomaterial is a great option for this. Carbon nanomaterial has a high potential for automated sensors due to their inherent properties. Low-dimensional carbon structures have a high surface area that is ideal for sensing [36–38]. Unlike polycrystalline materials such as metal oxides, quasi-dimensional carbon materials have no grain boundaries, making the sensor long-term stable. Some carbon materials, such as carbon nanotubes and graphene, have high-quality crystal lattices, so load carriers in these structures move at high speeds while generating little noise [39–42]. Since these two factors play a critical role in creating conductivity properties, it is easier to control and understand the surface chemistry of low-dimensional materials and high-quality crystal structures. Single crystal nanostructures are a great option for studying computational chemistry [43–45]. The sensitivity and selectivity of carbon materials can be manipulated by various methods, for example, structural defects and the creation of functional groups at the surface of nanotubes can be used for this purpose [46–48]. The Carbon nanotubes can be used to build various implements used in various ways. Low-cost methods such as lithography are suitable for making these devices. The mechanical properties of carbon nanotubes allow them to be used in flexible electronic devices [49, 50]. Another advantage of carbon nanotubes is the high cost-sensitivity ratio, which is high even at room temperature [51–53]. The low energy consumption of carbon nanotube-based devices allows them to operate independently and without the need for an external charger [54]. The movement of electronic signals in a chemical environment has advantages over optical methods; For example, the cost of these methods is low and their output is high, and in addition to simplicity, they are portable [55, 56]. Fullerenes are compounds with unparalleled electrical conductivity, high tensile strength, optical and thermal properties. The antimicrobial properties of fullerenes are among the recent findings of researchers. Fullerenes are almost insoluble in water. However, some soluble derivatives of fullerenes have significant antimicrobial effects. Fullerenes can form stable nanoparticle suspensions called nc60, which have stronger antimicrobial effects. Polyhydroxylated fullerenes [C60(OH)*n*], known as fullerenes, have stronger antimicrobial activity and less toxicity than nc60 [57–60].

In this review article, the use of carbon materials in the to construct various high-performance gas sensors is discussed, and its strengths and weaknesses are evaluated.

2 Carbon nanomaterial

Over the past few years, much research has been done on the use of carbon nanomaterial in the manufacture of sensors. More recently, graphene, as one of the new carbon allotropes, is overtaking carbon nanotubes in sensor construction [61–65]. But carbon nanomaterial is not limited to graphene and nanotubes, so structures such as nanoparticles, nanofibers, and Nano porous carbon materials can also be classified in this section. One of the most important reasons for the interest in making sensors from carbon nanomaterial is that these materials, in addition to having a regular nanoscale tubular structure, also have considerable stability; so they are very stable even when they are not functional [66–68]. Although there are a wide range of nanomaterial, their reactive chemistry is similar: organic chemistry. Before examining the use of carbon nanomaterial in electric gas sensors, we will briefly discuss the properties and production methods of some of these nanomaterial [69–71]. Figure 1 shows Schematic illustration of individual allotropes of Carbon nanotubes.

2.1 Carbon black

Black carbon is pure carbon within the sort of colloidal particles produced by the strategy of incomplete combustion or thermal decomposition of gaseous or liquid hydrocarbons under controlled conditions [72–75]. The physical

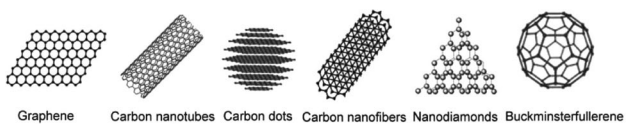

Fig. 1 Schematic illustration of individual allotropes of carbon nanomaterial [1–5]

appearance of this substance is black and it exists within the variety of powder or granules. Most carbon within the world is produced by both furnace and warmth methods, of which furnace carbon is that the most typical. During this method, very heavy aromatic oils are used as staple [76–78]. Under controlled conditions, the oil is heated in a very furnace and atomic number 6 is produced at specific pressures and temperatures. To do this, the oil evaporates and after pyrolysis turns into carbon micro particles. In most furnace reactors, the reaction rate is controlled by the flow of water or vapor [79–82]. The produced carbon is taken out of the reactor and cooled, and eventually packed after passing through a filter. Various gases, like CO and hydrogen, remain within the process. Most soot factories use a number of these residual gases to get heat, steam, or electricity [83–86]. Within the heating method, gas is employed to provide soot, and compounds like heavy aromatic oils or methane are used because the primary feed of this method. During this method, two separate furnaces are usually accustomed produce C, so the stuff enters the second furnace (carbon black production) 5 min after leaving the primary furnace (initial heating) [87–93]. Fossil fuel is injected into a hot furnace and within the absence of air, the oil decomposes to C. Aerosols produced by the flow of vapor were taken out of the system and trapped within the filters [94–96]. Various processes could also be accustomed purify and separate the unwanted compounds during this method so the output product is packaged. The hydrogen produced by this method will be wont to heat the second furnace. smut is physically and chemically quite distinct from soot, a substance during which quite 97% of its structure is clustered. Carbon encompasses a high extent, in order that its area is quite thousand g/cm^3 and its cavity dimensions are but 50 nm [97–100]. The density of lampblack is way under the theoretical density of graphite (2.25 g/cm^3). Figure 2 shows a high resolution image of a transmission microscope (TEM).

2.2 Carbon nanofibers

Vapor phase-grown carbon nanofibers (VGCNF) are carbon nanoscale fibers that are formed from hydrocarbon gases on metal catalysts such as nickel, iron, and cobalt at high temperatures (900–1500 °C) [101–105]. These hollow fibers are tubular in shape and grow from a primary graphite core 20–60 nm in diameter on the surface of the catalyst. The thickness of these nanofibers can be increased by using additional layers created by CVD method [106–112]. Subsequent layers are added to SP^3 hybridizing carbon on the nanofiber wall. The diameter of these nanofibers varies from 60–70 nm to 200 nm and their length can be from 1 to 100 nm [107, 108, 110, 111, 113, 114]. On the other hand, carbon nanofibers can be obtained in various controlled conditions with low cost and high growth rate using electro spinning method. A polymer such as polyacrylate (PAN) is used as the carbon source [115, 116]. This polymer is combined with suitable solvents and heated to a temperature below the boiling point and then used as a polymer solution in the electro spinning process. This solution is injected into a rotating tube using a special syringe. Voltage is applied between the syringe and the tube, which are a few centimeters apart [117–121]. The produced material is heat treated for several hours at a temperature of 300–400 °C. The product is then calcined and carbonized in the absence of oxygen (in an argon or nitrogen atmosphere) at 700–1000 °C [122–126]. The final product will be carbon nanofibers with a diameter of 40–400 nm and a length of over 70 microns (Fig. 3).

2.3 Carbon nanotube

There are different carbon allotropes; the carbon atoms in diamond have a tetrahedral lattice arrangement. In graphite, the carbon atoms are in the form of hexagonal sheets, and in graphene and fullerene, the atoms are arranged in a spherical or tubular manner [127–130]. Carbon nanotubes

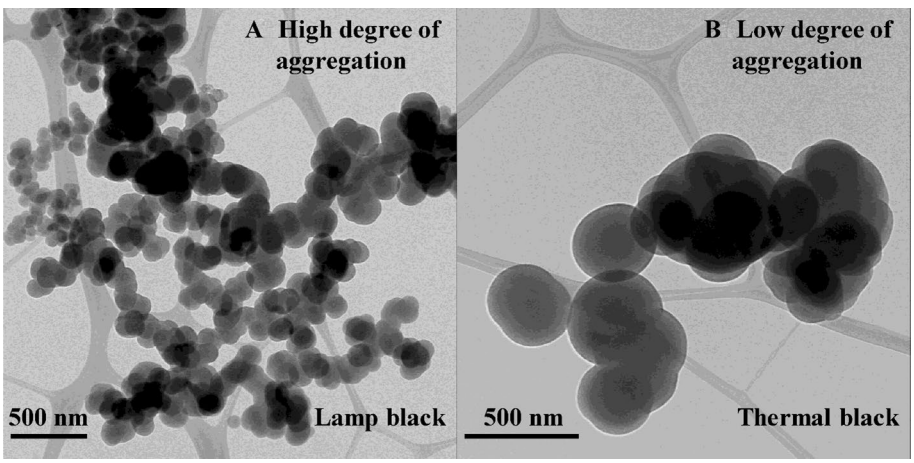

Fig. 2 Transmission electron microscope photos showing a high (**A**) and low (**B**) degree of accumulation in various carbon blacks [2]

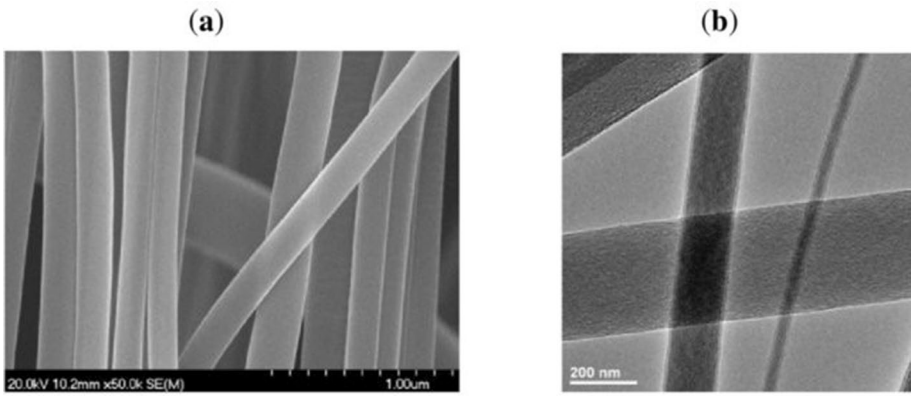

Fig. 3 SEM and TEM images showing the morphology of carbon nanofibers obtained by electro spinning [3–10]

have a fullerene-like structure that can be closed at the end [131–135]. The name of these nanostructures is derived from their physical shape in which graphene tubular sheets with different tubing angles lead to tubes with different symmetries [136, 137]. The angle of tubing and the radius of the tube determine the appearance of metal or semiconductor properties in these nanostructures. Nanotubes are divided into single-walled carbon nanotubes (SWCNTs) and multi-walled carbon nanotubes (MWCNTs) [138–141]. In multi-walled nanotubes, several graphene sheets are tubed. Carbon nanotubes naturally adhere to each other due to the van der Waals effect. These nanotubes are bonded together using a Sp^2 bond, similar to the interaction between graphite layers. The Sp^2 bond is stronger than the Sp^3 bond and is a bond between alkanes and diamonds, resulting in the unique structural strength of the nanotubes. Such strong bonds reduce the activity of nanotubes with surrounding molecules. Therefore, functionalization of carbon nanotubes is a suitable tool to improve the sensitivity and selectivity of nanotubes in the construction of gas sensors. Carbon nanotubes are produced using various methods, such as CVD, laser irradiation and discharge. Carbon nanotubes were first seen in 1991 among graphene soot products from discharge. In this process, the carbon in the negative electrode is sublimated due to the high temperature in the discharge process [142–144]. Since this method was first used to synthesize nanotubes, it is known as the most common method of producing carbon nanotubes. In this method, the yield of the product has been 30% by weight, which includes both types of nanotubes, single-walled and multi-walled, with lengths of up to 50 microns containing structural defects. In the laser irradiation process, a laser is used to evaporate graphite and an inert gas is used to conduct these vapors into the tank. Carbon nanotubes grow on the cold surface of the reactor. This method, developed by Smiley et al., Is suitable for the production of multi-walled carbon nanotubes [142–149]. The team used graphite composite and metal catalyst particles (a combination of cobalt and nickel) to synthesize single-walled carbon nanotubes. The efficiency of this process is 70% and its main product is single-walled carbon nanotubes. The diameter of these nanotubes is completely controllable and the diameter of the nanotubes can be controlled as desired by changing the temperature [150–153]. A research team used the catalyst-assisted CVD method to produce carbon nanotubes. During the CVD process, a layer of metal catalyst particles, generally nickel, cobalt, and iron, was used to produce carbon nanotubes [58–60]. CVD is a common method for the commercial production of carbon nanotubes [58–156]. In this method, the diameter of the nanotubes is related to the dimensions of the metal particles. The diameter of the nanotubes can be controlled by substrate patterning, heat treatment and plasma catalyst etching. In this method, gases such as nitrogen, hydrogen and ammonia are injected into the tank and the temperature reaches 700 degrees, then carbon-containing gases such as acetylene, ethylene, ethanol and methane are blown into the tank [157, 158]. These gases are broken down by heat, and the carbon atoms attach to the edge of the catalyst metal particles, and the growth of carbon nanotubes begins. Catalyst particles can stick to the tip of nanotubes and stick with them, depending on the type of catalyst used. If a strong electric field is used to grow carbon nanotubes, the nanotubes will grow in the direction of the applied field [158–161]. By adjusting the geometric shape of the reactor, the nanotubes can be grown vertically (so that they grow perpendicular to the substrate). Without field application, the growth of nanotubes occurs randomly in different directions. However, under certain conditions, nanotubes can be grown as dense, high-density vertical arrays to achieve a forest-like or carpet-like structure [162–164, 235–239]. Among the various methods of producing carbon nanotubes discussed in this article, laser irradiation is the most expensive and the least efficient method of producing carbon nanotubes. Therefore, the CVD method is the best option for the industrial production of carbon nanotubes [165–168, 240–242]. The reason for this is the low cost-to-income ratio, as well as the possibility of vertical growth of nanotubes on the desired substrate. Carbon nanotube growth sites must be carefully placed on the surface.

Figure 4 shows a picture of multi-walled carbon nanotubes grown to 50 microns by CVD with 95% purity. The thickness of the outer and inner layers of these nanotubes is 3–15 and 3–7 nm, respectively. In this image, the nanotubes are randomly oriented to create a porous material-like structure. Figure 4 shows Schematic structure and TEM images of single-walled carbon nanotubes and Multi-Walled Carbon Nanotubes [67–69].

2.4 Graphene

Kostya Novoselov et al. [81, 82] showed that the material had interesting electrical properties. Graphene has a high electrical conductivity due to its quality crystal structure. Electrical gap band, type of charge carriers and density of charge carriers can be changed in graphene; this can be done by applying different gate voltages to the substrate. Some of the properties of graphene make it a good choice for building a gas sensor [169–172]. Because graphene is two-dimensional and the entire surface of the material is in contact with the environment, graphene has the highest surface area per unit volume. The high conductivity of this material causes its conductivity to be similar to that of metals, and its Johnson noise is very low, while the presence of a few extra electrons changes the concentration of charge carriers [173–176]. This grapheme can be transferred to other substrates. The main challenge of growing graphene in CVD is that it is not possible to precisely control the number of layers grown, and also metal contaminants originating from the metal substrate enter the product. Figure 5 is a graphene micrograph taken using a modified TEM image.

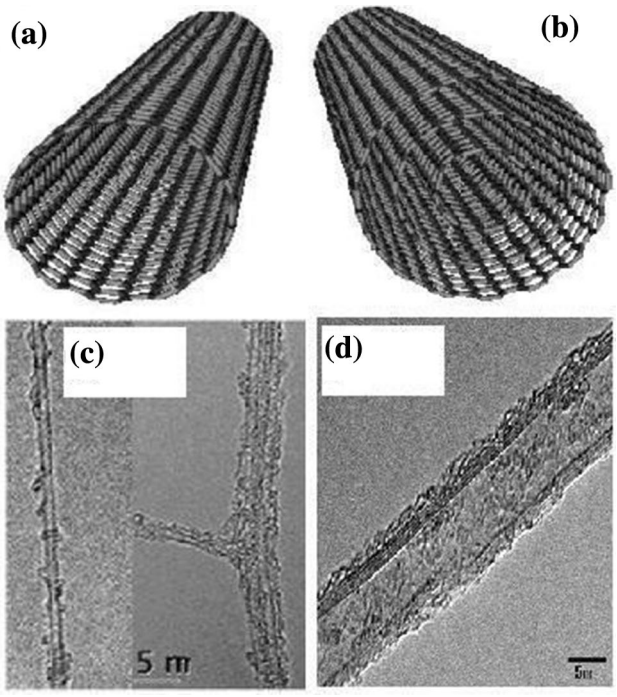

Fig. 4 Schematic structure and TEM images of single-walled carbon nanotubes and multi-walled carbon nanotubes. **A** Schematic structure of single-walled carbon nanotubes and **b** multi-walled carbon nanotubes. The transmission electron microscope (TEM) images of a **C** single-walled carbon nanotubes and **d** multi-walled carbon nanotubes [42]

2.5 Magnetron sputtering method of C-based nanostructured materials

Magnetron sputtering catholic sputtering of target material in magnetron discharge plasma allows obtaining thin films and coatings on various supports. Dutch physicist F. Penning was the primary to suggest using magnetron sputtering for the film deposition as early as 1935. Material sputtering in magnetron discharge was studied in several laboratories within the 1960s and within the 1970s various configurations of magnetron sputtering systems (MSS), including prototypes of recent planar magnetrons, were proposed. Industrial application of this technology started at the tip of the 1970s. Since then high-power impulse systems are designed additionally to DC and RF classical variants. Development of recent magnetrons is continuous now. Method of catalytic layers' deposition by magnetron sputtering has been developed and surface Raney catalysts and new effective catalysts for various processes are synthesized. Development of those works resulted within the creation of catalytic

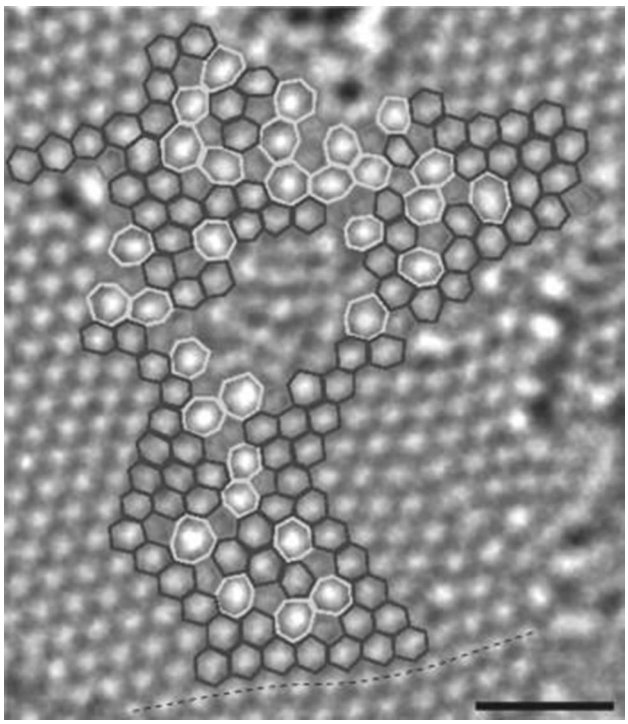

Fig. 5 Micrograph of graphene atomic structure [31, 32]

membrane reactors [177–179]. Carbon supports were considered closely: coating deposition added catalytic properties and improved thermal and chemical stability. Solving some problems important for hydrogen energy development (e.g. encapsulation of hydride forming powders, synthesis of catalysts on granules) needs various films/coatings (including Pt, Pd ones) on disperse carriers. Shortly new devices for prevention of powder aggregation were designed. Preliminary experiments on deposition of Cu and Ni on carbon powders showed the likelihood of carbon nanomaterials and carbon based nanocomposites coating [155].

3 Gas sensors with carbon nanomaterial

Various properties of carbon nanomaterial, such as optical and electrical properties, have led to the use of these materials to build sensors [180–182]. The different properties of graphene in a liquid medium, including pH sensors, heavy ions, have led to the use of these materials to make sensors. This review article is limited to the construction of gas sensors that change the electric current passing through them due to the target material [183, 184].

3.1 Carbon-black gas sensors

In these sensors, the carbon block is dispersed inside an insulating polymer, providing electrical conductivity to the film. If the desired gas/vapor is present, the polymer swells and eventually the electrical conductivity/resistance of the polymer changes. Using a suitable solvent, the viscosity of the polymer/carbon block is adjusted optimally, and then the polymer is patterned on the surface of the filter electrode. Various methods are applied to place the polymer on the surface of the electrodes, such as spin coating and droplets, and finally the coating dries. Changes in the strength of a composite in terms of carbon block percentage are explained using the theory of percolation (penetration) [185, 186]. If the amount of carbon black is low, the composite will be insulated due to the lack of connection between the conductive particles in the composite body. As the amount of carbon block in the polymer increases, the electrical resistance of the polymer decreases exponentially [74–77]. By increasing the concentration of carbon block and reaching the transfer point, the connection is established based on the penetration limit. If the desired vapor/gas is present, the polymer swells and the amount of electrical conductivity/resistance changes, this change is used to identify the gas. This mechanism is shown in Fig. 6. Lewis and colleagues used arrays of elements to respond to different vapors. The team used different polymer/carbon black composites to do this.

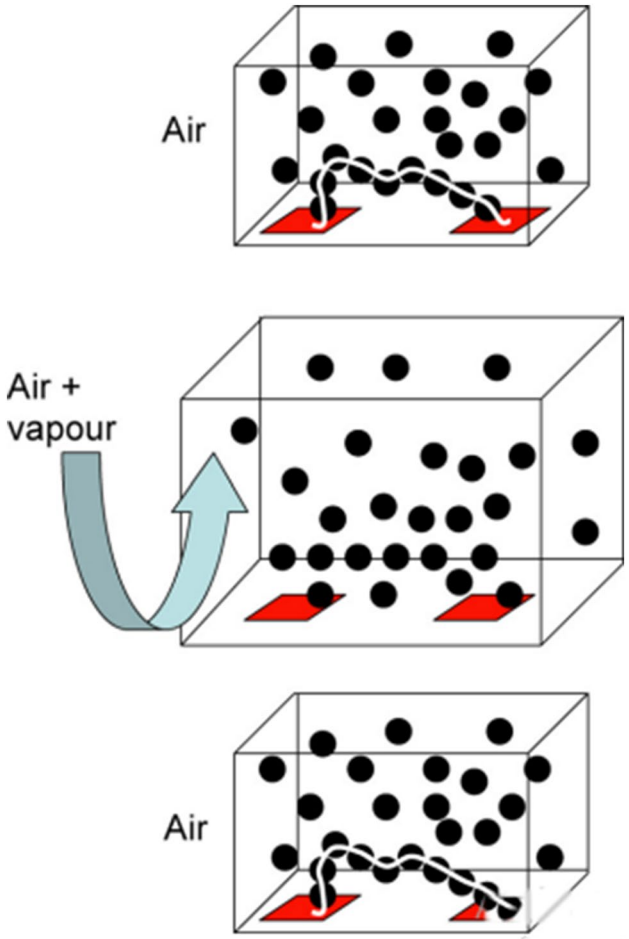

Fig. 6 Gas sensing mechanism of polymer/carbon black composite. Carbon black is dispersed in the polymer matrix. White line that the image above shows the conduction path between the electrodes gives. In the presence of vapors, this path is changed and the direction changes. If vapors are removed from the environment the steering wheel returns to its original position [33, 37]

Electrical resistance signals are output from these arrays and evaluated using a standard system [187–189]. The aim is to detect the presence of various vapors from organic solvents. This strategy can be combined with various software and hardware systems, and finally provide a small and compact tool with low cost and ease of use. For example, the sensory responses in the detection of benzene and methanol are shown in Fig. 7. In the presence of high concentrations of these toxic fumes, the responses obtained will be moderate. Polymer/carbon composite sensors may be delayed in responding to external stimuli due to aging of the polymer matrix or displacement of carbon black particles. Particle displacement or matrix aging causes a diffusion path [78–80]. This change in arrangement occurs as a result of repeated swelling and shrinkage of the polymer matrix due to repeated use of the sensor.

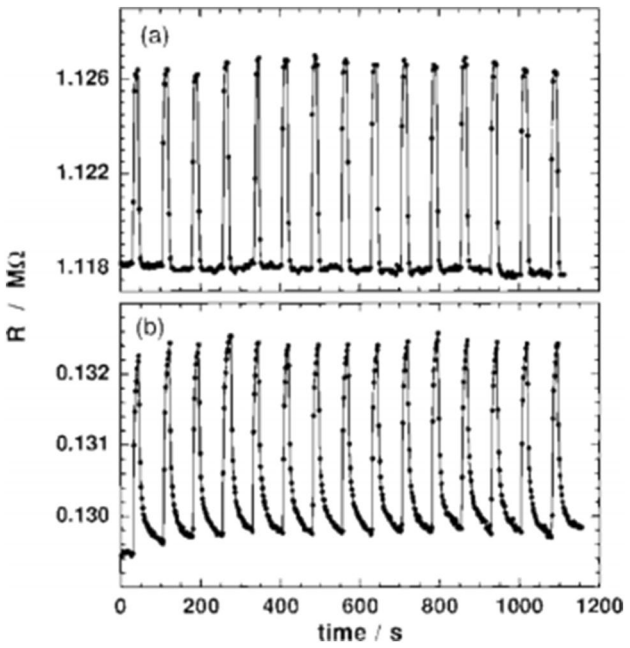

Fig. 7 Resistance of carbon black composite to **a** polyethylene-co-vinyl Acetate (**b**) poly (N-vinylpyrrolidone) in the presence of benzene and methanol. These compounds are alternately reduced and increased to repeatability and stability Examined [38]

3.2 Carbon nanofiber-based gas sensors

To overcome the instability problem of polymer/carbon black composites, Fu et al. [40] proposed the use of carbon nanofibers in polymers. As the polymer matrix absorbs the vapor, the viscosity of the matrix decreases and its volume increases. Under these conditions, carbon black nanoparticles accumulate in the polymer matrix. However, with the addition of polymer nanofibers, the vapor sensitivity in the polymer is improved and if vapor is adsorbed and desorbed from the composite, the nanofibers are resistant to displacement within the polymer due to their high surface-to-height ratio [190–193]. As a result, the main electrical penetration path in these composites is maintained after vapor absorption. A research team dispersed carbon nanofibers grown from the vapor phase into toluene and added it to polystyrene. This was done under mechanical rotation conditions. Figure 8 shows the SEM micrograph in composite films. The response and return cycle for tetrahydrofuran vapors can also be seen in this image.

Lee et al. [41] proposed an electro spinning method for fabricating polyacrylonitrile/carbon black complexes for use in gas sensors. This method is easily generalizable for mass production and inexpensive. Electro spinning fibers are exposed to heat treatment to form carbon fibers. These fibers are chemically activated to obtain active sites for gas absorption. KOH solution is used as an activating agent, which improves the structure and increases the specific surface area of carbon fiber by almost 100 equal. As a result, the amount of gas absorbed increases dramatically. The surface of the sample is also modified using fluoridation operations. The applied functional groups increase the gas absorption to the sensor surface. Adding some carbon black also improves electrical conductivity. In total, chemical activation, the presence of carbon black and fluoridation operations improves the sensor response to nitrous oxide and carbon monoxide by up to 5 equal.

Fong et al. [42] proposed a method for producing carbon nanofibers adorned with Pd nanoparticles that used electro spinning to produce fibers and more chemically to functionalize. These materials are completely uniform and the product of this process is carbon nanofibers with a diameter of 300 nm on which Pd nanoparticles are spread. The dimensions of Pd nanoparticles will be from a few nanometers to a few tens of nanometers.

Surface functionalization is achieved by immersing electro spun polyacrylonitrile fibers in aqueous NH_2OH solution. The functionalized surface is immersed in Pd $(NO_3)_2$ solution so that the amid oxime functional groups can absorb Pd_2 + ions. The compound is immersed in NH_2OH solution to allow Pd nanoparticles to adhere to the surface. In the next step, the polymer surface is heat treated to carbonize and stabilize. The same method can be used to produce carbon nanofibers decorated with different metal nanoparticles. Electro spun nanofibers are completely flexible and do not change when exposed to hydrogen at room temperature [194, 195]. Sensors made with this method have a good response in a hydrogen-containing environment and the speed of response and return to the original state is acceptable in them. The activity of the sensor surface is highly dependent on the dimensions of the metal clusters attached to the fiber surface, and this method can lead to the proper distribution of Pd clusters on the fiber surface [196].

Jang et al. [43] proposed a method for producing electro spun carbon nanofibers decorated with metal oxides. The advantage of this method is that the nanofibers are coated with metal oxide by an extractable method. To create metal oxides (ZnO and SnO_2) on the surface of carbon fibers, nanofibers with shell core structure (PAN) (PVP) were produced as the starting material. To create these structures, two injection needles should be used in electro spinning; the reason for this is the incompatibility of the two polymers. The root of the incompatibility of the two polymers is the difference in the inherent physical properties of the polymers, especially their viscosity. By decomposing the PVP phase, very small hybrids of CNFs are created, which eventually lead to the conversion of metal precursors ($ZnAc_2$ and $SnCl_4$) to metal oxide nanostructures. Also, during the heat treatment process, PANs are converted to 40 nm CNFs. The morphology of metal nanostructures can be controlled

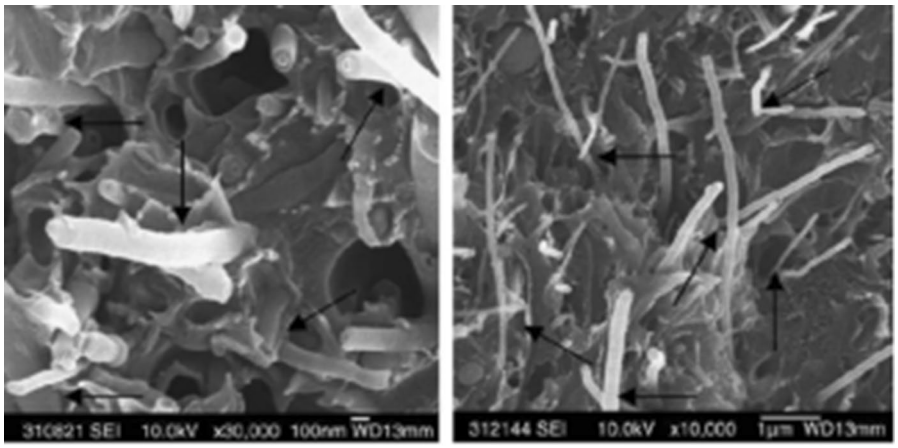

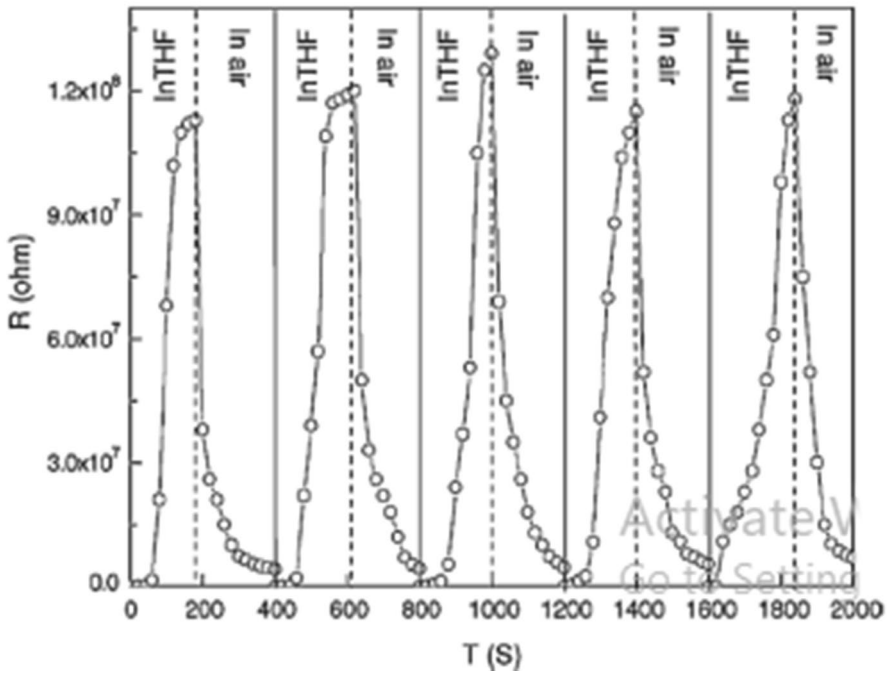

Fig. 8 Micrograph of carbon nanofibers grown to form gives a polystyrene composite. Percentage of nanofibers 25.6 Percentage by weight [upper left (and 5.12% by weight) high right Is. The arrow indicates the point of contact between the fibers Creates a bridge in this network. Electrical response Composite 25.6% by weight at 35 °C In the presence of water vapor and tetrahydrofuran vapor is seen [40]

by varying the concentration of the precursor in the PVP solution. Nanofibers coated with metal oxide are introduced into the ethanol solution and exposed to ultrasonic; then, using the spin coating method, it is placed on the electrode arrays to measure their conductivity. These sensors were tested in the presence of dimethyl methyl phosphonate (DMMP) at room temperature. The minimum detection level of hybrid carbon nanofibers is 0.1 parts per million (ppm). This high sensitivity is due to the presence of metal oxide nanostructures on the surface of carbon nanofibers, which increases the surface area and the tendency of DMMP to vapors. However, the effect of ambient humidity on the responses in this sensor has not yet been discussed. Figure 9 shows SEM images with high and low resolution of carbon nanofibers decorated with various metal oxides. The normalized response to different concentrations in air is also shown.

3.3 Carbon nanotube-based gas sensors

The electronic properties of carbon nanotubes are highly sensitive to the chemical environment around the nanotubes. This sensitivity is a suitable tool for using nanotubes in the sensor sector.

Dai et al. [44] produced semiconductor single-walled carbon nanotubes using the CVD growth method on a SiO_2/Si substrate. By connecting a wire to the nanotubes and creating a metal/nanotube/metal structure, the team was able to build a transistor that could change direction due to different voltages. The electrical conductivity of these nanotubes was investigated in the presence of ammonium vapors and nitrogen dioxide [197–199]. The single-walled carbon nanotube used in this study was a cavity-reinforced semiconductor. The results showed that due to

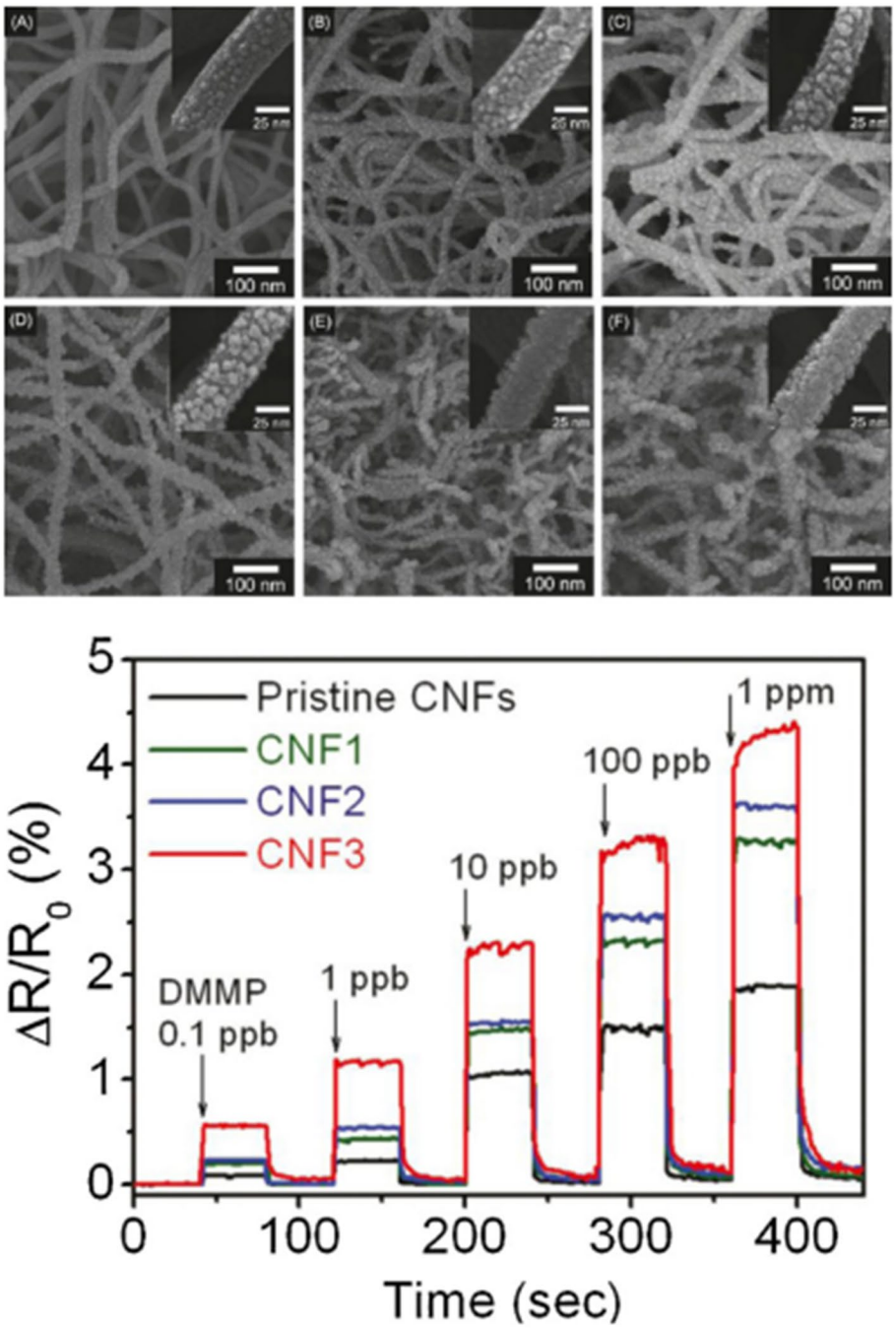

Fig. 9 High image: FESEM images with high resolution power from $SnCl_4$ in PVP solution ZnAc2 and Carbon nanofibers in the presence Concentrations **a** 0.5, **b** 0.75, **c** 1, **d** 1.25, **e** 1.5 and **f** 2 Weight percent is showing. The image below shows the normalized resistance changes in Indicates the presence of DMMP vapors [43]

the application of positive gate voltage to this system, the electrical conductivity is reduced three times. Figure 10 shows the electrical response of the single-walled carbon nanotube device to gaseous molecules. In the presence of ammonia gas, the nanotube capacity band moves away from the Fermi surface, which reduces the number of cavities and thus the conductivity. In the case of nitrogen dioxide, the presence of this gas transfers the form energy level of the nanotube to the capacitance band. This increases the concentration of pores in the nanotube, resulting in improved electrical conductivity. The researchers studied the effect of nitrogen dioxide and ammonia gas on the electrical properties of a Single walled carbon nanotube -based sensor. The response of single-walled carbon nanotube forests is less than that of single nanotube devices [200–203]. This result can have two reasons: In bulk single-walled carbon nanotube samples, the effects of molecular interaction are less than in metal and semiconductor nanotubes. Also, inner tubes in single-walled carbon nanotube filaments are not able to interact with gases; this

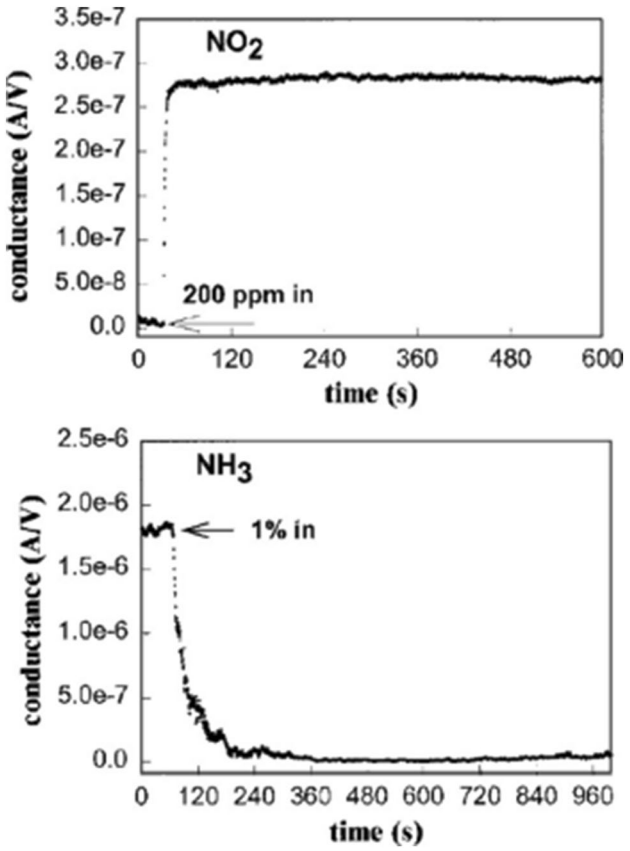

Fig. 10 Electrical response of semiconductor nanotubes in the presence of molecules Gas with a flow of 200 ppm of NO_2 and SWNT-S in the presence of Al flow with 1 weight percentage of NH_3

is because molecules cannot penetrate the single-walled carbon nanotube strands [204–206].

Zatt et al. [45] found that single–walled carbon nanotube was highly sensitive to oxygen. Adding a small amount of oxygen to these nanotubes can reverse their electrical resistance, so semiconductor nanotubes can turn into metal nanotubes in the presence of oxygen. The authors of the paper stated that carbon nanotubes could be used as chemical gas sensors, but that the surrounding air could affect some of the intrinsic properties of these nanotubes. Finally, the team concluded that the charge transfer caused by oxygen to the nanotubes is a sign of structural defects in the nanotubes, and that the entry of oxygen into the nanotubes and their adsorption into the inner wall of the nanotubes should not be overlooked.

Goldoni et al. [47] investigated the relationship between gas sensing properties and defects and contaminants on the surface of single-walled carbon nanotubes. The team investigated the effects of oxygen, nitrogen, carbon monoxide, moisture, nitrogen dioxide, sulfur oxide and ammonia gases on the emission spectrum of nanotubes before and after vacuum heat treatment. Heat treatment on nanotubes reduces the number of structural defects in nanotubes, which are caused by purification or removal of contaminants such as catalyst particles. After heat treatment, the electronic spectrum of single-walled carbon nanotubes loses its sensitivity to oxygen, nitrogen, carbon monoxide and moisture, while it is sensitive to ammonia, nitrogen dioxide and sulfur oxide. Thus, some of the imagined intrinsic properties of pure nanotubes or those that are slightly heated are affected by contaminants, defects, or catalytic particles. The authors of this paper found that gas molecules in the presence of air (i.e., oxygen, nitrogen and moisture) have a weak interaction with nanotubes, i.e,. they do not form any chemical bonds with nanotubes. Therefore, in order to achieve high sensitivity in these sensors, the surface of the nanotubes must be clean and its structural defects must be controlled.

Some studies show that functionalizing the side wall of nanotubes leads to better bonding of specific compounds with nanotubes and also improves the sensitivity and selectivity of nanotubes. For example, carbon nanotubes with a coating of palladium are sensitive to hydrogen. The concept of metal–carbon nanotube cluster hybrids as a sensitive material with a site for adsorption of different target molecules was introduced in a theoretical study [207–210]. In this study, which was studied on CNT-AL clusters, the researchers showed that by absorbing ammonia, charge accumulation and polarization occurred in the area between the aluminum cluster and the nanotube. This load transfer provides important information about the electronic response of the system. This affects the ionic portions of the bonds and changes the position of the Fermi energy level. Therefore, changing the electrical conductivity of the CNT-Al system is used as a measure of the sensitivity of chemical sensors. Based on these theoretical results, the metal/CNT cluster hybrid can be used to identify chemical species with high sensitivity and selectivity. A key point in the strategy is to use nanoclusters that can absorb or release large amounts of charge in the presence of the target molecule. Therefore, these nanoclusters will affect the electron transfer in the nanotubes. This strategy was first proposed by several research groups in 2006 and 2007.

Kumar et al. [52] Used chemistry to create platinum-coated carbon nanotubes to produce a hydrogen-sensitive sensor.

Star et al. [53] selectively placed elements such as Pt, Pd, Au, Rh, Sn, Mg, Fe, Co, Ni, Zn, Mo, W, V, and Cr onto carbon nanotubes to provide a sensor for carbon monoxide, nitrogen dioxide, and methane and produce hydrogen sulfide, ammonia and hydrogen. One of the challenges of this path is to be able to place metals of the same dimensions on the wall of the nanotube. If the particles are not fixed on the surface of the nanotubes, they will move and the sensor response will be unstable. Figure 11 shows this problem for metal-coated carbon nanotubes. For these

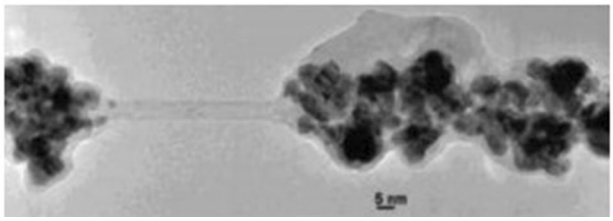

Fig. 11 TEM micrograph of carbon nanotubes coated with Pd nanoparticles. The decoration is done with the selected plating method

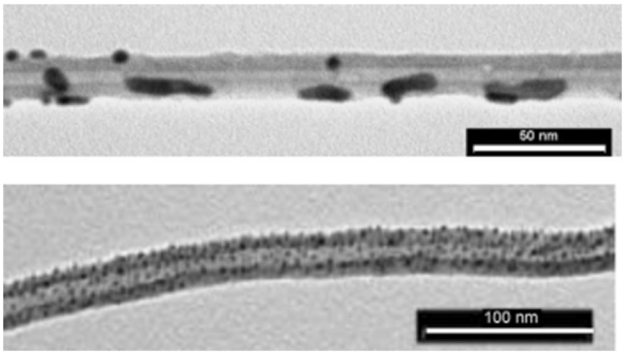

Fig. 12 Micrograph of multi-walled carbon nanotubes decorated with gold nanoparticles. Gold particles it is mobile and is applied on the obtained nanotubes and gold nanoparticles they are evenly distributed and located on the defective points. This nanotube using Plasma is activated

nanotubes, plating method with selected position has been used. This problem can be solved by adopting a method of operating cold active plasma, such as oxygen plasma on nanotubes. This approach allows nanomaterial engineers and designers to produce hybrid nanostructures in a single step, without the need for steps such as activation, functionalization, or cleaning. The plasma method allows to control the shape, dimensions, coordination and penetration of metal nanoparticles on nanotubes. Figure 12 shows the plasma operation that causes the nanoparticles to settle uniformly on the wall of the nanotubes. Metal atoms are not stationary and are constantly moving, these atoms continue to move until they reach the nucleus. The oxygen plasma method can create different nuclei on the nanotube. This was previously predicted using computational studies. In addition, oxidation operations affect the density states of the capacitance bands and increase the working function of pure nanotubes. The working function of nanotubes treated with oxygen plasma is very close to metals such as platinum, gold, palladium and nickel. This facilitates the movement of electrons between nanoparticles and nanotubes. The direction of charge movement depends on the surrounding gaseous environment. The interaction between nanoparticles and nanotubes

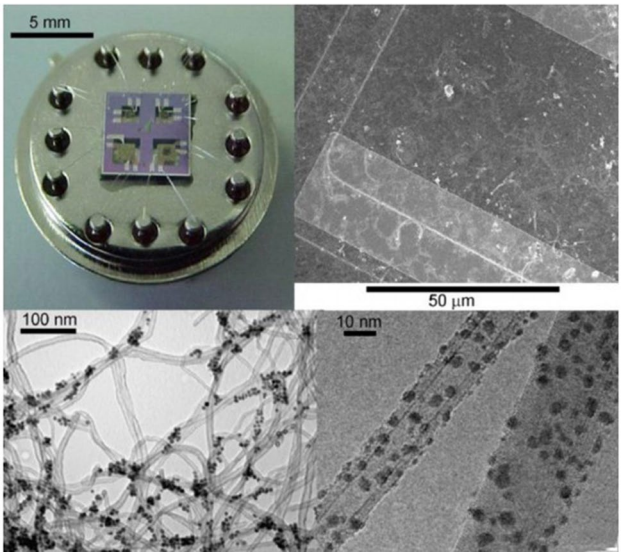

Fig. 13 Optical microscope image of a 4-element sensor array. The image SEM of the electrode representing the bridge created by the CNT. TEM image of Pd coated nanotubes and image of Rh-coated nanotubes

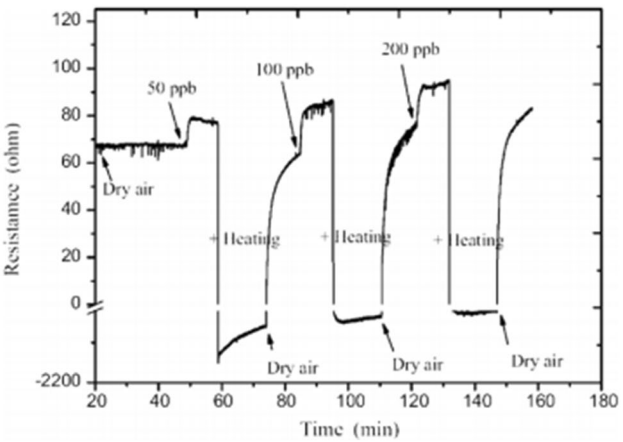

Fig. 14 Curve of response and reduction in CNT-Rh sensors. These sensors at room temperature and in Operated at a temperature of 150 °C

facilitates the identification of gases by nanotubes, which is done by changing the electrical conductivity of hybrid nanomaterial.

Haick et al. [73] identified benzene using plasma-processed arrays. In this study, researchers used metal-walled multi-walled carbon nanotubes. The limit of benzene measurement was less than 50 ppb and the detection process was performed by changing the humidity in the presence of disturbing species such as carbon monoxide, hydrogen sulfide and nitrogen dioxide. Figure 13 shows a

four-element sensor. Figure 14 shows the response of an Rh-walled multi-walled nanotube sensor to benzene.

Penza et al. [62–64] used the sputtering method to decorate the nanotubes with Au, Pt, Pd, Ru, and Ag particles. Plasma method helps to functionalize the products obtained from sputtering. This method has been used successfully to functionalize nanotubes grown in CVD, without the need to transfer the nanotubes to another device for functionalization. Researchers have developed sensors to detect nitrogen dioxide, ammonia, hydrogen, hydrogen sulfide and carbon monoxide. Although few studies have been performed on metal cladding of nanotubes, this method is frequently used to improve the selectivity of nanotubes. When the ratio between plasma nanotubes and metal oxide is appropriate, hybrid sensors can perform well at room temperature, allowing the detection of carbon monoxide and nitrogen dioxide in the ppm concentrations. These optimized sensors are less sensitive to the negative effects of moisture. There have been few successes in enhancing nanotube replacement to increase the sensitivity and selectivity of nanotubes. The addition of boron and nitrogen can improve the electrical conductivity of nanotubes. Nitrogen-reinforced carbon nanotubes are highly efficient in identifying hazardous gas molecules due to the presence of pyridine sites on the surface of the nanotubes. The researchers found that nitrogen-reinforced nanotubes had a very short reduction time for ammonia detection. These nanotubes also respond very strongly and reversibly to ethanol. Various studies have shown that no charge exchange occurs between carbon monoxide and nanotubes. However, calculations show that it is possible to use reinforced carbon nanotubes to detect carbon monoxide. Various researchers have investigated the modification of nanotube walls with organic molecules to improve their sensitivity.

Johnson et al. [83] Showed that sensors based on religious strings can perform well. In these sensors, the world is used as an identification site. The researchers showed that these sensors were able to react to the smell of explosive gases and nerve toxins, something that is not seen in pure nanotubes. These sensors can be used to detect and quantify gases if they have a specially sequenced diode.

Penza et al. [62–64] investigated the sensory properties of Porphyrin/carbon nanotube films. They investigated the possibility of changing the absorption effect of the Porphyrin layer to change the strength of the nanotube layer. The presence of porphyria films increases the selectivity of the electrical resistance of nanotubes to volatile compounds. This is due to the high efficiency of metal-coated Porphyrin in transferring charge from adsorbent molecules to nanotubes. The researchers suggested that the selectivity of these sensors could be improved by using different metal compounds in the body of the Porphyrin. One of the main problems

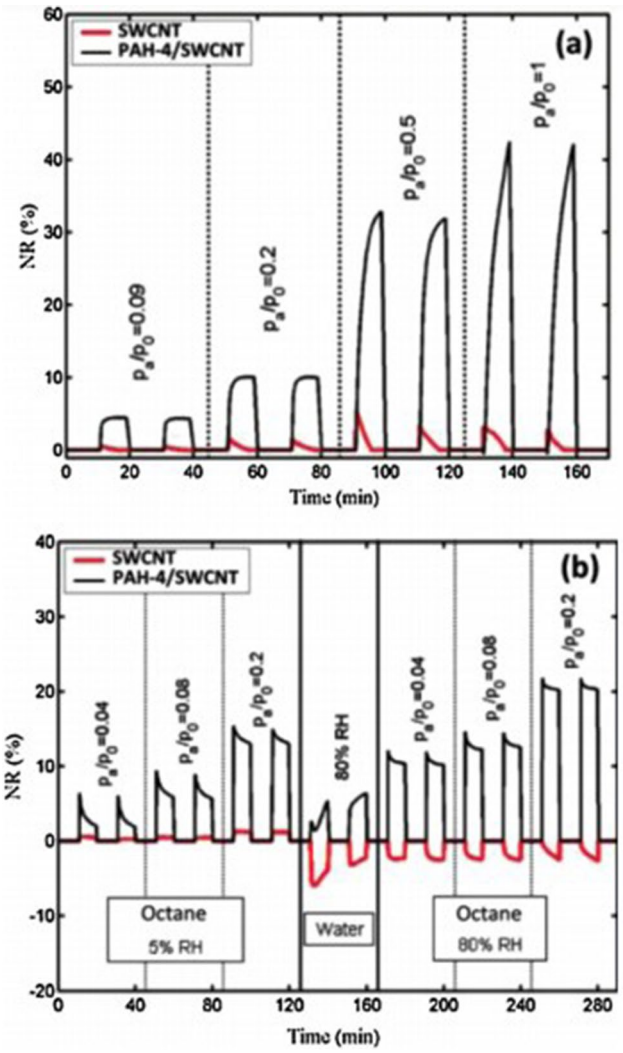

Fig. 15 Sensory response to different concentrations of **a** hexanol in dry air. **b** Acetone in dry air and humidity 80%. Red curve: response generated by a single-walled carbon nanotube sensor. Black curve: the response generated by the carbon nanotube sensor PAH functionalized single wall

in the commercialization of these nanotube sensors is the changes in humidity in the environment.

Novoselov et al. [80, 81] came up with an interesting idea to solve this problem. They poured a drop of purified single-walled nanotube onto a silicon surface and made nanotube electrodes. These electrodes were coated with polycyclic aromatic hydrocarbon compounds (PAHs). PAHs have alkyl groups that can self-assemble into large, electron-rich molecular groups that can guarantee good charge transfer. Nanometer-thick PAH columns easily form a three-dimensional, spongy structure with a high volume-to-surface ratio. Multi crystalline PAH layers are formed on the surface of nanotubes by casting. Using the right combination of PAH and SWNT, an accurate sensor with high selectivity can be

developed that can distinguish polar organic volatile compounds from non-polar ones, so that the ambient humidity can vary from 5 to 80% (Fig. 15). These findings show that the research process is moving towards the construction of inexpensive, lightweight, low-consumption and non-destructive sensors that are able to identify a wide range of volatile organic materials in our environment.

Liu et al. [87] Used single-walled carbon nanotubes with amino phenyl and amino Cyclodextrin functional groups to identify organic contaminants. These sensors are able to detect organic contaminants, and in the presence of these contaminants, there are drastic changes in their electrical conductivity. Star Group recently developed a single-walled carbon nanotube-based sensor using copper complex that can selectively detect 0.5 ppm ethylene.

When single-walled carbon nanotubes are used as field-effect transistors in nano sensors, they have high selectivity and low energy consumption. These nanotubes can be used in various devices, but due to the presence of impurities, a purification process must be applied on them. When field-effect transistors operate in ambient conditions (ie, variable ambient humidity), the device undergoes a great deal of stress [211–214].

Kaner et al. [86] proposed a method in which individual nanotubes grow directly between the non-metallized parts of the device. Pd is then layered on this structure using shadow masks. This new system can work without stress in different humidity. This finding opens a new path for highly sensitive nano sensors containing intact carbon nanotubes.

4 Methods of making grapheme

4.1 Mechanical delamination method

This method, which is the first method of making graphene, involves separating graphene sheets from natural graphite with HOPG (Fig. 16). Separating graphene sheets from each other using glue is possible and is a simple, inexpensive, yet low-efficiency, randomly generated plate production method [215, 216, 257–260]. In this method, after gluing graphite pieces together several times and reducing the number of layers, finally the adhesive tape containing graphene plates can be transferred on a 300 nm substrate of silicon and using light microscope, AFM or Raman spectroscopy microscope, the number and distribution of layers (Figs. 17, 18, 19). Identified graphene. The better the structural structure of the original graphite and the larger the dimensions, the larger and less flawed the detached graphite plates will be. The highest quality graphene for research studies with a mobility of about 40,000 $cm^2\ v^{-1}\ s^{-1}$ for carriers, but due to the random results and uncontrollable efficiency in obtaining graphene components is practically not capable

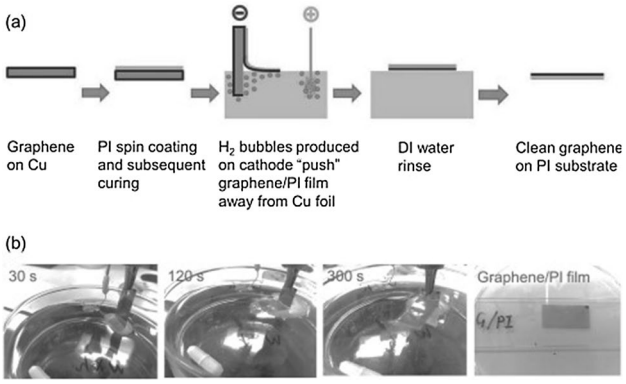

Fig. 16 **a** Image of direct delamination of graphene onto polyimide substrate. Throughout the operation, no sacrificial Poly (methyl methacrylate) help is used. **b** Direct delamination time-lapse optical images; the whole process takes 5 min [95–97].

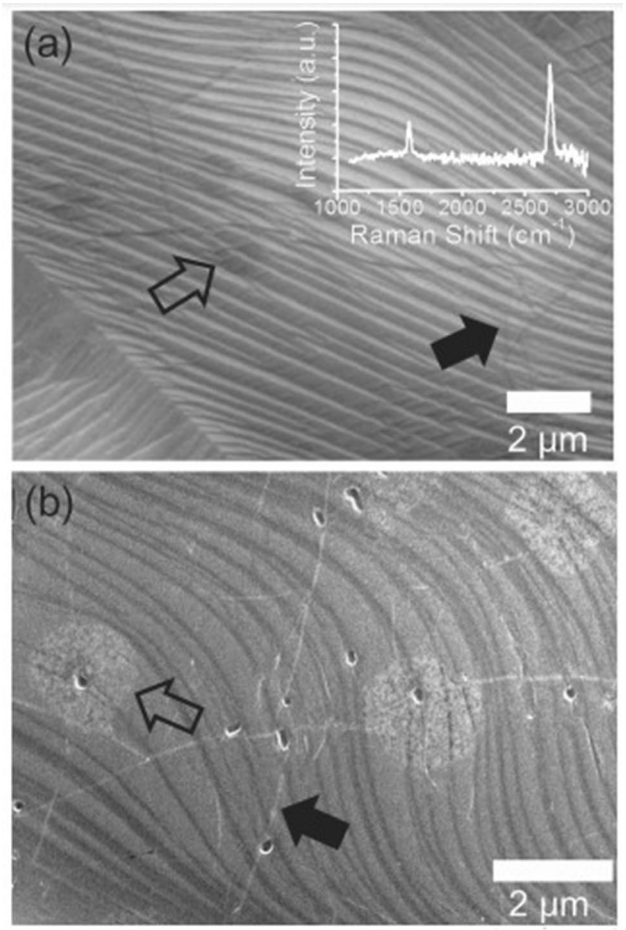

Fig. 17 SEM photographs of CVD-grown graphene **a** prior to direct delamination (on Cu) and **b** after direct delamination (on polyimide) [95–97]

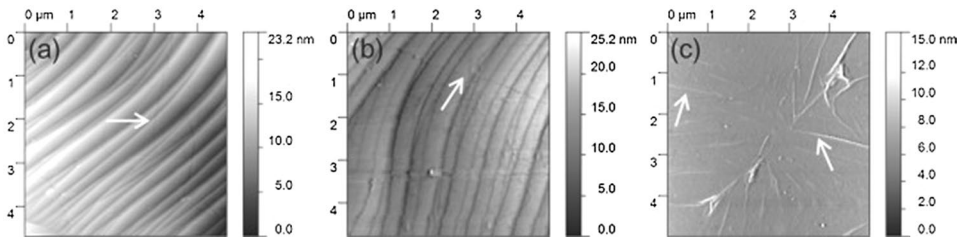

Fig. 18 AFM photographs of graphene **a** grown on Cu, **b** directly delaminated with polyimide support/substrate, and **c** delaminated onto a prepared polyimide substrate with poly (methyl methacrylate) [95–97]

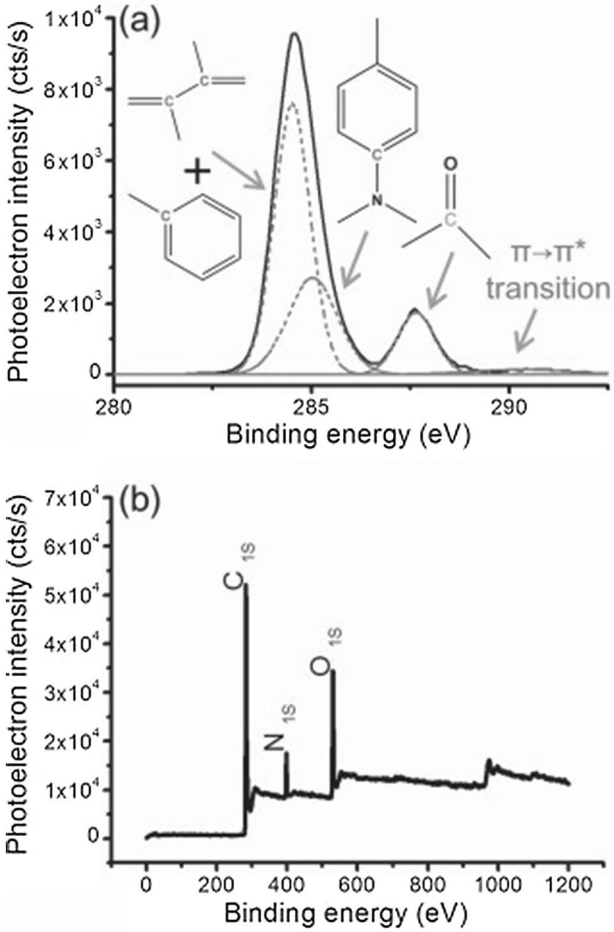

Fig. 19 **a** Specifically delaminated graphene XPS C 1 s spectrum on a polyimide backing there's also a Gaussian/Lorentzian fit. The various peaks in polyimide and graphene lead to different carbon atom bonding configurations. **b** There are no inorganic chemicals in the XPS survey spectrum (at the threshold detection limit) [95–97]

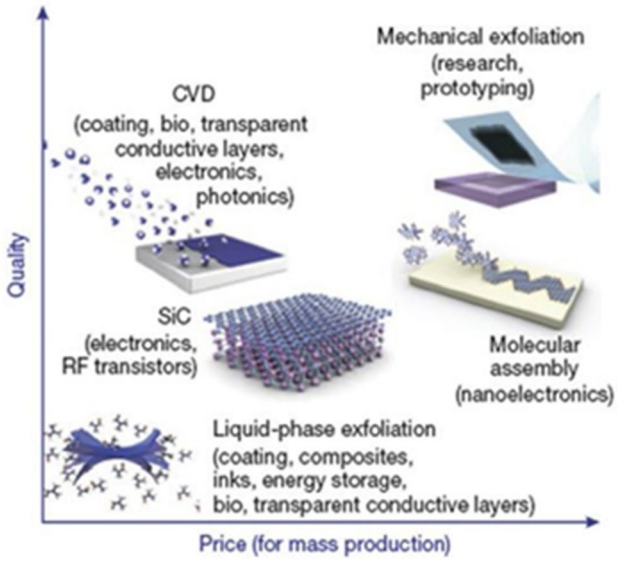

Fig. 20 Demonstration of different manufacturing methods and comparison between quality and mass production capability of each [95–97]

of large-scale industrialization. Figure 20 shows a variety of manufacturing methods and a comparison between quality and mass production capabilities of each [95–97, 261, 262].

4.2 CVD chemical vapor deposition method

In this method, a hydrocarbon is decomposed as a carbon source and a layer or layers of graphene are grown on the metal substrate. Since this method has an acceptable speed of production, good quality, and the possibility of mass production, it has been considered since 2010. The metal layer, which is usually composed of nickel, copper [98] and other intermediate metals such as Pd [98], Pt [100], Rh [101], and Ir [102], acts as a catalyst in the formation of carbon covalent bonds. The presence of grains and defects in the metal substrate is transferred to graphene, and the resulting graphene is a kind of polycrystalline, and the mobility of the carriers is of the order 15,000 $cm^2 v^{-1} s^{-1}$.

4.3 Chemical method

This method involves oxidizing the graphite layers and so permeating the oxidized layers as graphene oxide. Hammers in 1958 [104] was ready to provide an optimal method for oxidation of graphite using acid and permanganate. By weakening the van der Waals bonds between the plates in grapheme within the oxidation process, the space between the plate's increases to 0.75–0.65 nm. In grapheme oxide, the oxidation groups of sp^2 hybridization convert graphene to sp^3 and introduce a special inventory, especially

electrically. Graphene oxide reduction means the removal of oxide groups and therefore the recovery of sp2 hybridization, referred to as Reduced Graphene Oxide (RGO), which is 4 or 5 times less electrically resistant than grapheme oxide. This method, while cheap and mass-produced, may be a colloidal candidate for industrial applications, especially within the fields of polymer composites and hybrid nanostructures. However, the tiny size (between 1 and 5 microns) of the plates and therefore the presence of oxide residual groups and structural defects because of oxidation processes and reduction of electrical mobility of order $1cm^2\ v^{-1}\ s^{-1}$, which is not recommended for electronic and transistor applications. Figure 20 provides a comparison between graphene manufacturing methods in terms of quality and production capacity, which may be a summary of this section [217–219].

4.4 Graphene-based sensors

In 2007, Shedin et al. [105] were able, as the first grapheme sensor report, to absorption and desorption the gas molecule from HOPG laminated graphene without any physical or chemical activation and only by removing the contaminants deposited on the graphene during electrode fabrication. This group was able to measure the presence of electron accepting gases such as I2, NO_2, and NH_3 and electron donor gases such as NO, H_2O, and CO in the controlled conditions (2 ppb) (Fig. 21). From the Hall Effect test, Shedin et al. [105] Proved that the presence of electron acceptor (donor) gases leads to the injection of a cavity (electron) of the order of 1012 cm^2 into grapheme. Gas absorption causes the dispersion of carriers from these additional injected loads, which according to the report of this group, in comparison with the reduction of carrier mobility due to impurities, the effect of change in the density of charge carriers is dominant [220–222]. The group also attributed the oscillations and steps in the dynamic response of an electric current to the absorption and desorption of gas molecules. One of the challenges of grapheme sensing is the absorption of gaseous molecules that require energy and do not occur spontaneously due to the active carbon level of grapheme. For graphene obtained from sensor mechanical sheet up to 25ppt in the presence of NH_3, NO and NO_2 gases have been reported [106, 250–252]. The interesting thing about this work is the use of UV rays during the desorption process. UV radiation in the presence of oxygen leads to the production of reactive oxygen species, which clean the graphene surface and facilitate the adsorption process. It is unlikely to have a clean and unpolluted graphene after the manufacturing process. The presence of these residual contaminants on the graphene surface can act as a sensitizer and improve its sensitivity to the clean sample. In a report, Johnson Group [107, 253–256] showed that the presence of polymers left over from the manufacturing process can act as an adsorbent and improve the sensor one or two times, because after removing these polymer contaminants by heating the process in Ar/H_2 at 400 °C. The mobility of the carriers increases fourfold and the density of the contaminated loads decreases by one-third and their sensitization decreases by one or two times. Other polymers such as PMMA (Poly methyl methacrylate) and PANI (Polyaniline) have a similar effect on graphene. The use of three-dimensional graphene structures grown by CVD on porous nickel and copper foams is a novel way to make graphene sensors [108, 109]. These foams act as a mold and catalyst for the growth of graphene and are removed with a chemical solution after growth. This three-dimensional graphene network has a large surface area (Fig. 22) and is electrically and mechanically interconnected. Because the graphene mesh may collapse after removing the metal foam, the PMMA polymer layer is used as a backing.

Robinson et al. [110, 111, 243–246] in their first study on RGO sensors in 2008 showed that both regions with sp^2 and sp^3 orbitals (graphene domains and graft defects) play an important role in the sensor [247–249]. In this report, GO plates were placed on metal electrodes as a network of interconnected plates and the sensor response of the

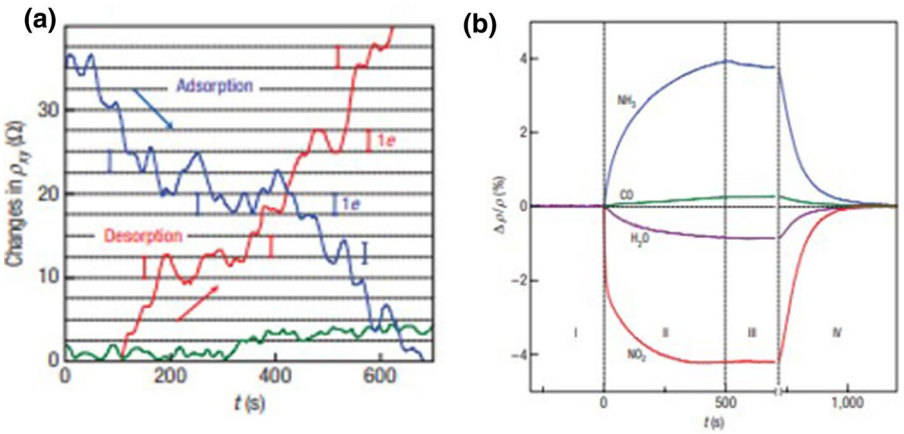

Fig. 21 **a** Dynamic response to other gases such as electron donors and electron acceptors and **b** the effect of absorption and desorption of a gas molecule on the electrical resistance of grapheme [105]

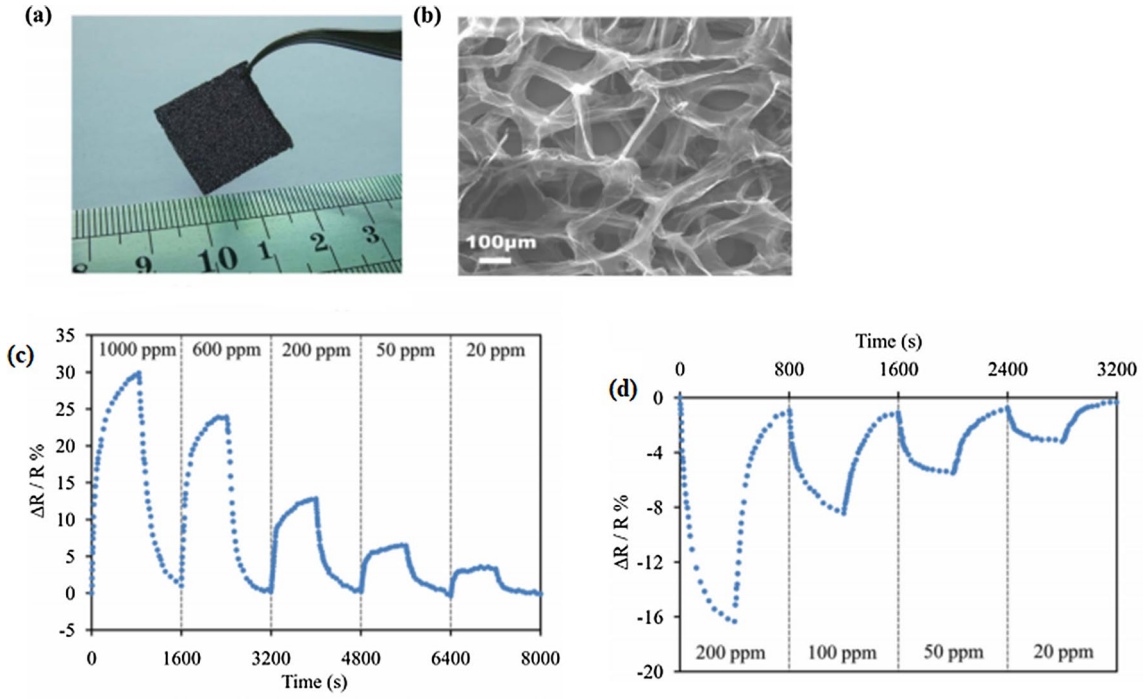

Fig. 22 **a**, **b** The three-dimensional structure of graphene and its sensory response behavior to **c** NO_2 and **d** NH_3. During desorption, 400 K heating is applied [108]

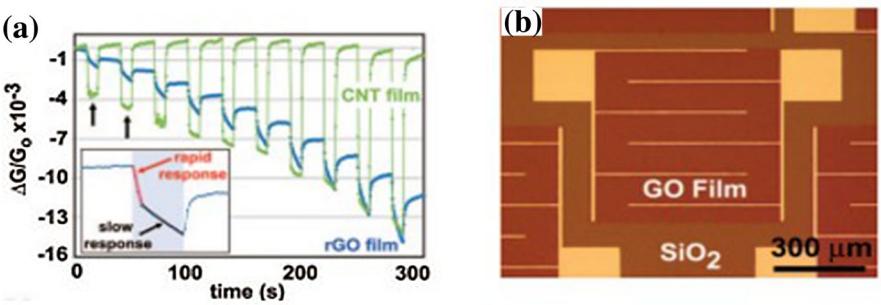

Fig. 23 **a** The structure of the electrodes and the RGO layer on it, **b** Comparison of the sensor response of RGO and nanotubes to acetone [110].

samples with different reduction times was investigated (Fig. 23). According to the findings of this group, the rate of graphene reduction affects the noise and gas sensitivity, because with increasing the rate of reduction of graphene and areas with sp^2 hybridization, less response and adsorption times were observed [263]. Therefore, it can be said that areas with sp^2 orbital are low energy locations for rapid gas adsorption and adsorption, while slower absorption and desorption occur with stronger binding in sp^3 and defective areas. The group showed that by increasing the thickness of the RGO layer, the amount of electrical noise is also reduced compared to nanotubes, and to study the selectivity of four toxic gases such as CEES, DMMP, HCN and DNT were tested.

5 Gas sensors based on graphene oxide-metal two-component structures

Catalytic metals like platinum (Pt) and palladium (Pd), when placed on RGO plates, form a weak Schottky barrier when properly interacted with. This Schottky barrier depends on the function of the metal and the way it interacts with the graphene plate. This Schottky barrier dam is incredibly sensitive to gas absorption and injection of carriers and results in many relative changes in current and voltage for instance, during a report on the Pd-RGO hybrid structure, [112, 223, 224] a Schottky barrier dam is formed of type n, and with the presence of gas and interaction with Pd, the metal working function changes, leading

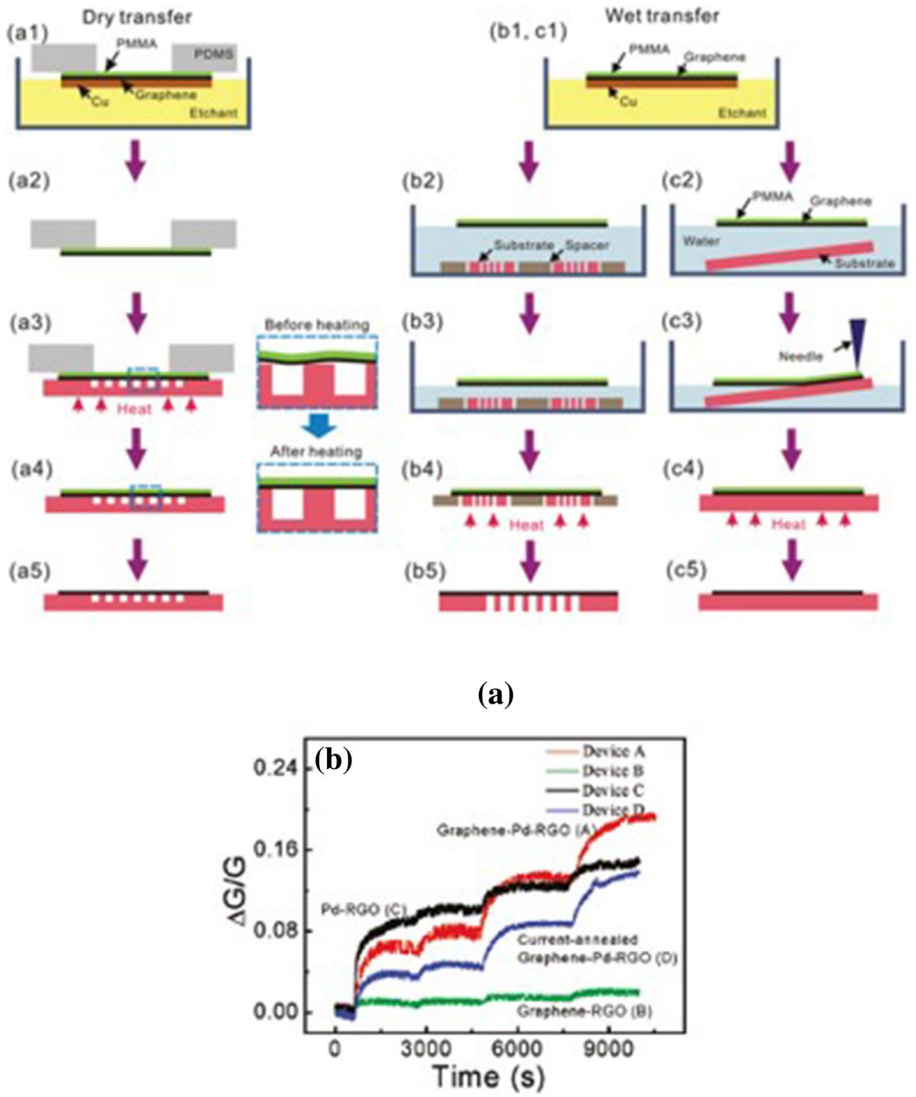

Fig. 24 **a** Stages of construction of Pd-RGO hybrid structures and design of Schottky dam formed in the interphase and **b** Sensor results for NO gas [112]

to a decrease in Schottky barrier dam height and a rise in flow. (Fig. 24). On the opposite hand, NO, as a gasified, can exchange charge with the hybrid system and increase conduction. Table 1 shows the reports on graphene-metal oxide hybrid sensors.

6 Gas sensors based on graphene oxide-metal oxide two-component structures

Many of the existing and well-known sensors are metal oxide based sensors, also known as solid state sensors.

Table 1 The reports on graphene-metal oxide hybrid sensors

Hybrid material	Structure type synthesis method	Gas type and sensitivity	Operating temperature	Refs
Zno/RGO	Chemical	NO, NH_3, CO, 10 ppm	RT	[107]
WO_3/RGO	Chemical	Ethanol, 500 ppm	300 °C	[108]
WO_3/RGO	Hydrothermal	NO_2, 10 ppm	300 °C	[113]
ZnO_2/RGO	Hydrothermal	Propanl, 100 ppm	300 °C	[110]
ZnO_2/RGO	Chemical	NO_2, NH_3, 20 ppm	300 °C	[111]
Cu_2O/RGO	Chemical	H_2S, 1 ppm	RT	[114]

The basis of these sensors is the absorption of oxygen groups as O^{2-}, ^{-}O and O^{-2} on the surface and the change of the Schottky barrier between the metal oxide boundaries. By absorbing these oxygen groups as lethal electron groups (with high electronegativity), the metal oxide of one electron participates and traps electrons from the surface to the trap levels of the resulting electron trap [115, 225, 226]. This migration of electrons from the surface to the mass creates an empty layer of electrons on the surface, especially in the grain boundaries, and the width of this layer increases with the absorption of more oxygen groups. However, the presence of grapheme as a good conductor with a suitable working function can play an important role in sensing hybrid structures with metal oxides [227–229]. In general, the effects of the presence of RGO plates on a metal oxide hybrid structure can be divided into three categories: increased electrical conductivity of the hybrid layer due to the good conductivity of graphene plates; Semiconductors with a gap band greater than 1 eV usually have high electrical resistance at room temperature, and the presence of graphene plates as fast flow channels can provide adequate conductivity for the sensor at lower temperatures [116, 117]. Graphene itself can act as a sensory component and increase the sensitivity of the hybrid layer when the whole surface of graphene isn't coated with metal oxide nanostructures. When the area of graphene is high, grapheme forms a typical bond with metal oxide as a substrate [230–234]. The charge exchange between grapheme and metal oxide is restricted to those areas and also the potential barrier in these areas is additionally very sensitive to gas absorption [118, 119]. Therefore, the amount and type of active sensor sites and sensor sensitivity increases with the presence of graphene. Figure 25 shows a diagram of the mentioned maps. In fact, graphene in a very hybrid layer practically creates more and more sensitive areas for gas access by improving the conduction, increasing and modifying common seasons, the width of the empty layers, and also the height of potential dams. On the opposite hand, graphene as a substrate can cause new nucleation on itself, thus reducing the further accumulation of metal oxide nanostructures and thus increasing the effective expanse of the layer. This effect, unlike CNTs, is restricted to the two-dimensional structure of graphene.

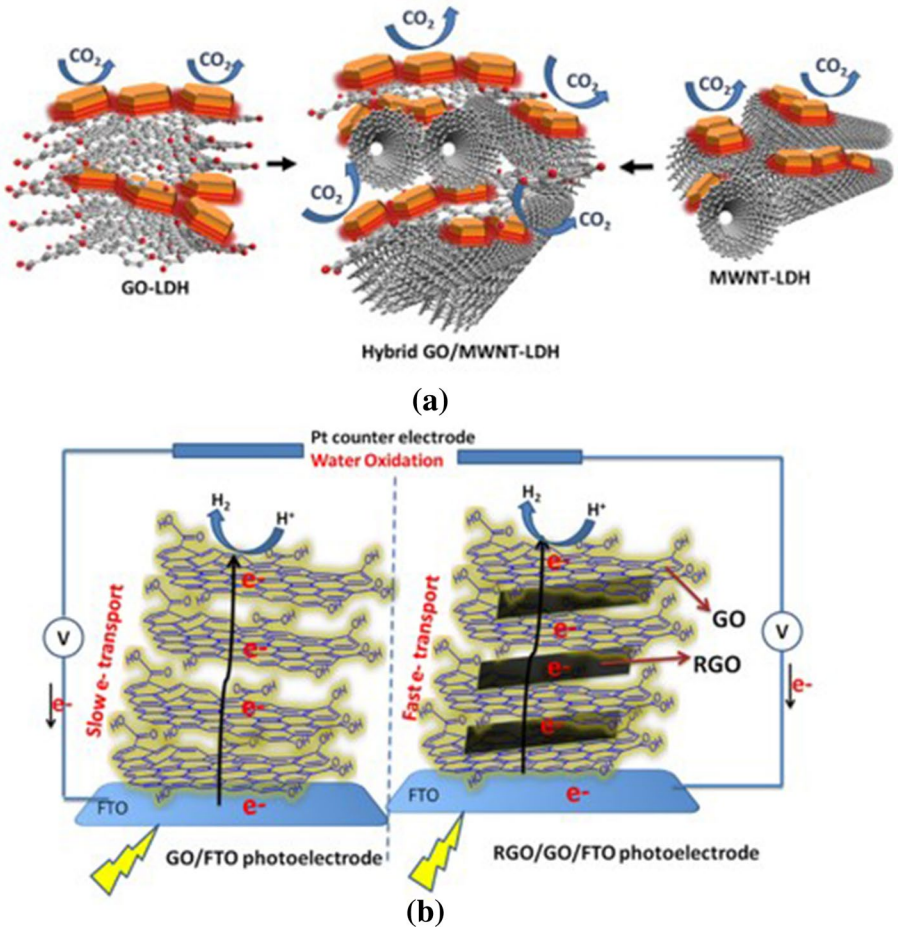

Fig. 25 **a** Scheme of the effect of the presence of grapheme in a hybrid layer with metal oxide, **b** Design in the absence of graphene in a hybrid layer with metal oxide [120, 121]

7 Conclusion and perspective

Over the years, many researchers have turned their attention to carbon nanomaterials. The unique optical, mechanical and electronic properties of these nanostructures have led them to use these nanomaterials to develop small devices, such as energy-saving sensors. In this review, we will cover the work on carbon nanotubes used in sensors. In particular, examples of carbon nanotubes that play a key role in devices that are sensors of biomolecules, gas, light and pressure changes. Carbon and graphene nanotubes are among the most important nanostructures used in industry. This is due to their extraordinary mechanical, electrical, thermal and optical properties. These nanostructures are widely used in the manufacture of items such as nanocomposites with special properties and electronic devices. For both of these nanostructures, there are many challenges in the controlled synthesis and economization of industrial production, and significant advances have been made over time. In case of producing controlled, quality and cheaper samples, these two nanostructures have a lot of potential for the evolution of many industries. Today, the unique electronic properties and structures of carbon nanostructures, such as nanotubes, regenerated graphene, and graphene oxide, are used to make sensors. However, the industrial and commercial production of these sensors is not yet successful and there is a need for improvements in this technology. The first challenge in this direction is to find a cheap way to mass produce these sensors. If pure carbon nanotubes or pure graphene are needed to make the sensor, the CVD growth method is the best choice. Although some studies have shown the production of very pure single carbon nanotubes with this method, due to the humidity of the environment, stresses occur on the nanotubes. Much research needs to be done on the growth of carbon nanotubes to establish predetermined metal or semiconductor properties in these nanostructures.

Supplementary Information The online version contains supplementary material available at https://doi.org/10.1007/s42823-021-00276-9.

Acknowledgements Department of Chemical Engineering, Arak Branch, Islamic Azad University, Arak, Iran

Young Researchers and Elite Club, Gachsaran Branch, Islamic Azad University, Gachsaran, Iran

Author contributions IR, HHK, ZHM: investigation, concept and design, experimental studies, writing–original draft, reviewing and editing, AAAA: investigation, concept and design, experimental studies, writing–original draft, reviewing and editing, AZI: investigation, concept and design, experimental studies, data curation, writing – original draft, reviewing and editing, EK: investigation, concept and design, data curation, conceptualization, writing–original draft, reviewing and editing.

Funding The funders had no role in the design of the study; in the collection, analyses, or interpretation of data; in the writing of the manuscript, or in the decision to publish the results.

Availability of data and materials All data generated or analyzed during this study are included in this published article.

Declarations

Conflict of interest The author declare that they have no competing interests.

Research involving human participants and/or animals This work does not contain any studies with human participants or animals performed by any of the authors.

Informed consent Informed consent was obtained from all individual participants for whom identifying information is included in this paper.

Consent for publication Not applicable.

References

1. Roberts ME, LeMieux MC, Bao Z (2009) Sorted and aligned single-walled carbon nanotube networks for transistor-baseds aqueous chemical sensors. ACS Nano 3:3287–3293
2. International Carbon Black Association (ICBA), www.carbon-black.org/.
3. Hughes TV, Chambers CR (1889) Manufacture of carbon filaments. US Patent 405: 480.
4. Tibbetts GG (1983) Carbon fibers produced by pyrolysis of natural gas in stainless steel tubes. Appl Phys Lett 42:666
5. Oberlin A, Endo M, Koyama T (1976) Filamentous growth of carbon through benzene decomposition. J Cryst Growth 32:335–349
6. Yu Y, Gu L, Zhu C, Van Aken PA, Maier J (2009) Tin nanoparticles encapsulated in porous multichannel carbon microtubes: preparation by single-nozzle electrospinning and application as anode material for high-performance Li-based batteries. J Am Chem Soc 131:15984–59851
7. Palmeri MJ, Putz KW, Brinson LC (2010) Sacrificial bonds in stacked-cup carbon nanofibers: biomimetic toughening mechanisms for composite systems. ACS Nano 4:4256–4264
8. Kim C, Jeong YI, Ngoc BTN, Yang KS, Kojima M, Kim YA, Endo M, Lee JW (2007) Synthesis and characterization of porous carbon nanofibers with hollow cores through the thermal treatment of electrospun copolymeric nanofiber webs. Small 3:91–95
9. Bazilevsky AV, Yarin AL, Megaridis CM (2007) Co-electrospinning of core–shell fibers using a single-nozzle technique. Langmuir 23:2311–2314
10. Xu X, Zhuang X, Chen X, Wang X, Yang L, Jing X (2006) Preparation of coresheath composite nanofibers by emulsion electrospinning. Macromol Rapid Commun 27:1637–1642
11. Peng S, Cho K (2003) Ab initio study of doped carbon nanotube sensors. Nano Lett 3:513–517
12. Iijima S (1991) Helical microtubules of graphitic carbon. Nature 354:56–58
13. Guo T, Nikolaev P, Rinzler AG, Tomanek D, Colbert DT, Smalley RE (1995) Self-assembly of tubular fullerenes. J Phys Chem 99:10694–10697

14. Guo T, Nikolaev P, Thess A, Colbert D, Smalley R (1995) Catalytic growth of singlewalled nanotubes by laser vaporization. Chem Phys Lett 243:49–54
15. José-Yacamán M, Miki-Yoshida M, Rendón L, Santiesteban JG (1993) Catalytic growthof carbonmicrotubules withfullerene structure. AppliedPhysics Letters 62:657
16. Ishigami N, Ago H, Imamoto K, Tsuji M, Iakoubovskii K, Minami N (2008) Crystal planen dependent growth of aligned single-walled carbon nanotubes on sapphire. J Am Chem Soc 130:9918–9924
17. Ren ZF, Huang ZP, Xu JW, Wang JH, Bush P, Siegal MP, Provencio PN (1998) Synthesis of large arrays of well-aligned carbon nanotubes on glass. Science 282:1105–1107
18. Novoselov KS, Geim AK, Morozov SV, Jiang D, Zhang Y, Dubonos SV, Grigorieva IV, Firsov AA (2004) Electric field effect in atomically thin carbon films. Science 306:666–669
19. Novoselov KS, Geim AK, Morozov SV, Jiang D, Katsnelson MI, Grigorieva IV, Dubonos SV, Firsov AA (2005) Two-dimensional gas of massless Dirac fermions in graphene. Nature 438:197–200
20. Castro EV, Novoselov KS, Morozov SV, Peres NMR, Dos Santos J, Nilsson J, Guinea F, Geim AK, Castro Neto AH (2007) Biased bilayer graphene: semiconductor with a gap tunable by the electric field effect. Phys Rev Lett 99:216802
21. Schedin F, Geim AK, Morozov SV, Hill EW, Blake P, Katsnelson MI, Novoselov KS (2007) Detection of individual gas molecules adsorbed on graphene. Nat Mater 6:652–655
22. Geim AK, Novoselov KS (2007) The rise of graphene. Nat Mater 6:183–191
23. Novoselov KS, Jiang D, Schedin F, Booth TJ, Khotkevich VV, Morozov SV, Geim AK (2005) Two dimensional atomic crystals. Proc Natl Acad Sci USA 102:10451–10453
24. Dutta P, Horn PM (1981) Low-frequency fluctuations in solids: 1/f noise. Rev Mod Phys 53:497–516
25. Park S, Ruoff RS (2009) Chemical methods for the production of graphenes. Nat Nanotechnol 4:217–224
26. Gomez-Navarro C, Weitz RT, Bittner AM, Scolari M, Mews A, Burghard M, Kern K (2007) Electronic transport properties of individual chemically reduced graphene oxide sheets. Nano Lett 7:3499–3503
27. Yang D, Velamakanni A, Bozoklu G, Park S, Stoller M, Piner RD, Stankovich S, Jung I, Field DA, Ventrice CA, Ruoff RS (2009) Chemical analysis of graphene oxide films after heat and chemical treatments by X-ray photoelectron and microRaman spectroscopy. Carbon 47:145–152
28. de Heer WA, Berger C, Wu XS, First PN, Conrad EH, Li XB, Li TB, Sprinkle M, Hass J, Sadowski ML, Potemski M, Martinez G (2007) Epitaxial graphene. Solid State Commun 143:92–100
29. Seyller T, Bostwick A, Emtsev KV, Horn K, Ley L, McChesney JL, Ohta T, Riley JD, Rotenberg E, Speck F (2008) Epitaxial grapheme. A new material. Phys Status Solidi B 245:1436–1446
30. Berger C, Song ZM, Li TB, Li XB, Ogbazghi AY, Feng R, Dai ZT, Marchenkov AN, Conrad EH, First PN, de Heer WA (2004) Ultrathin epitaxial graphite: 2D electrongasproperties and aroute toward graphene-based dnanoelectronics. J Phys Chem B 108:19912–19921
31. Kim KS, Zhao Y, Jang H, Lee SY, Kim JM, Ahn JH, Kim P, Choi JY, Hong BH (2009) Large-scale pattern growth of graphene films for stretchable transparent electrodes. Nature 457:706–710
32. Li XS, Cai WW, An JH, Kim S, Nah J, Yang DX, Piner R, Velamakanni A, Jung I, Tutuc E, Banerjee SK, Colombo L, Ruoff RS (2009) Large-area synthesis of high-quality and uniform graphene films on copper foils. Science 324:1312–1314
33. Norman RH (1970) Conductive rubbers and plastics. Elsevier, Amsterdam
34. Lundberg B, Sundqvist B (1986) Resistivity of a composite conducting polymer as a function of temperature, pressure, and environment: Applications as a pressure and gas concentration transducer. J Appl Phys 60:1074
35. Ruschau GR, Newnham RE, Runt J, Smith BE (1989) 0–3 ceramic/polymer composite chemical sensors. Sens Actuat 20:269–275
36. Talik P, Zabkowskawaclawek M, Waclawek W (1992) Sensing properties of the CB–PCV composites for chlorinated hydrocarbon vapours. J Mater Sci 27:6807
37. Kirkpatrick S (1973) Percolation and conduction. Rev Mod Phys 45:574
38. Lonergan MC, Severin EJ, Doleman BJ, Beaber SA, Grubbs RH, Lewis NS (1996) Array-based vapor sensing using chemically sensitive, carbon black–polymer resistors. Chem Mater 8:2298–2312
39. Doleman BJ, Lonergan MC, Severin EJ, Vaid TP, Lewis NS (1998) Carbonblack–polymer composite vapor detectors. Anal Chem 70:4177–4190
40. Zhang B, Fu R, Zhang M, Dong X, Wang L, Pittman CU (2006) Gas sensitive vapor grown carbon nanofiber/polystyrene sensors. Mater Res Bull 41:553–562
41. Im JS, Kang SC, Lee SH, Lee YS (2010) Improved gas sensing of electrospun carbon fiber based on pore structure, conductivity and surface modification. Carbon 48:2573–2581
42. Zhang L, Wang X, Zhao Y, Zhu Z, Fong H (2012) Electrospun carbon nano-felt surface-attached with Pd nanoparticles for hydrogen sensing application. Mater Lett 68:133–136
43. Lee JS, Kwon OS, Park SJ, Park EY, You SA, Yoon H, Jang J (2011) Fabrication of ultrafine metal-oxide-decorated carbon nanofibres for DMMP sensor application. ACS Nano 10:7992–8001
44. Kong J, Franklin NR, Zhou C, Chapline MG, Peng S, Cho K, Dai H (2000) Nanotube molecular wires as chemical sensors. Science 287:622–625
45. Collins PG, Bradley K, Ishigami M, Zett A (2000) Extreme oxygen sensitivity of electronic properties of carbon nanotubes. Science 287:1801–1804
46. Tan S, Verschueren A, Dekker C (1998) Room-temperature transistor based on a single carbon nanotube. Nature 393:49
47. Goldoni A, Larciprete R, Petaccia L, Lizzit S (2003) Single-wall carbon nanotube interaction with gases: sample contaminants and environmental monitoring. J Am Chem Soc 125:11329–11333
48. Kauffman DR, Star A (2008) Carbon nanotube gas and vapor sensors. Angew Chem Int Ed 47:6550–6570
49. Bondavalli P, Legagneux P, Pribat D (2009) Carbon nanotubes based transistors as gas sensors: state of the art and critical review. Sens Actuat B Chem 140:304–318
50. Kong J, Chapline MG, Dai H (2001) Functionalized carbon nanotubes for molecular hydrogen sensors. Adv Mater 13:1384–1386
51. Zhao Q, Nardelli MB, Lu W, Bernhoc J (2005) Carbon nanotubesmetal cluster composites: a new road to chemical sensors. Nano Lett 5:847–851
52. Kumar MK, Ramaprabhu S (2006) Nanostructured Ptfunctionalized multiwalled carbon nanotubes based hydrogen sensor. J Phys Chem B 110:11291–11298
53. Star A, Joshi V, Skarupo S, Thomas D, Gabriel JCP (2006) Gas sensor array based metal-decorated carbon nanotubes. J Phys Chem B 110:21014–21020
54. Ionescu R, Espinosa EH, Sotter E, Llobet E, Vilanova X, Correig X, Felten A, Bittencourt C, Van Lier G, Charlier J-C, Pireaux JJ (2006) Oxygen functionalisation of MWNT and their use as gas sensitive thick-film layers. Sens Actuat B Chem 113:36–46
55. Espinosa EH, Ionescu R, Bittencourt C, Felten A, Erni R, Van Tendeloo G et al (2007) Metal-decorated muliwall carbon nanotubes for low temperature gas sensing. Thin Solid Films 515:8322–8327

56. Charlier J-C, Arnaud L, Avilov IV, Delgado M, Demoisson F, Espinosa EH, Ewels CP, Felten A, Guillot J, Ionescu R, Leghrib R, Llobet E, Mansour A, Migeon H-N, Pireaux J-J, Reniers F, Suarez-Martinez I, Watson GE, Zanolli Z (2009) Carbon nanotubes randomly decorated with gold clusters: from nano2hybrid atomic structures to gas sensing prototypes. Nanotechnology 29:375501
57. Ago H, Kugler T, Cacialli F, Salaneck WR, Shaffer MSP, Windle AH et al (1999) Work functions and surface functional groups of multiwall carbon nanotubes. J Phys Chem B 103:8116–8121
58. Leghrib R, Felten A, Demoisson F, Reniers F, Pireaux J-J, Llobet E (2010) Room-temperature, selective detection of benzene attrace levels using plasmatreated metal-decorated multiwalled carbon nanotubes. Carbon 48:3477–3484
59. Leghrib R, Dufour T, Demoisson F, Claessens N, Reniers F, Llobet E (2011) Gas sensing properties of multiwall carbon nanotubes decorated with rhodium nanoparticles. Sens Actuat B Chem 160:974–980
60. Zanolli Z, Leghrib R, Felten A, Pireaux J-J, Llobet E, Charlier J-C (2011) Gas sensing with Au-decorated carbon nanotubes. ACS Nano 5:4592–4599
61. Leghrib R, Llobet E (2011) Quantitative trace analysis of benzene using an array of plasma-treated metal-decorated carbon nanotubes and fuzzy adaptive resonant theory techniques. Anal Chim Acta 708:19–27
62. Penza M, Cassano G, Rossi R, Alvisi M, Rizzo A, Signore MA, Dikonimos Th, Serra E, Giorgi R (2007) Enhancement of sensitivity in gas chemiresistors based on carbon nanotube surface functionalized with noble metal (Au, Pt) nanoclusters. Appl Phys Lett 90:173123
63. Penza M, Rossi R, Alvisi M, Cassano G, Signore MA, Serra E, Giorgi R (2008) Ptand Pd-nanoclusters functionalized carbon nanotubes networked films for subppm gas sensors. Sens Actuators, B Chem 135:289–297
64. Penza M, Rossi R, Alvisi M, Signore MA, Cassano G, Dimaio D, Pentassuglia R, Piscopiello E, Serra E, Falconieri M (2009) Characterization of metal modified and vertically-aligned carbon nanotube films for functionally enhanced gas sensor applications. Thin Solid Films 517:6211–6216
65. Espinosa EH, Ionescu R, Llobet E, Felten A, Bittencourt C, Sotter E, Topalian Z, Heszler P, Granqvist CG, Pireaux JJ, Correig X (2007) Highly selective NO2 gas sensors made of MWNTs and WO3 hybrid layers. J Electrochem Soc 154:J141–J149
66. Leghrib R, Pavelko R, Felten A, Vasiliev A, Cané C, Gràcia I, Pireaux J-J, Llobet E (2010) Gas sensors based on multiwall carbon nanotubes decorated with tin oxide nanoclusters. Sens Actuat B Chem 145:411–416
67. Hsu WK, Firth S, Redlich P, Terrones M, Terrones H, Zhu YQ, Grobert N, Schilder A, Clark RJH, Krotoa HW, Walton DRM (2000) J Mater Chem 1:1425
68. Villalpando-Paez F, Romero AH, Munoz-Sandoval E, Martinez LM, Terrones H, Terrones M (2004) Fabrication of vapor and gas sensors using films of aligned CNx nanotubes. Chem Phys Lett 386:137
69. Peng S, Cho K (2000) Chemical control of nanotube electronics. Nanotechnology 11:57
70. Santucci S, Picozzi S, Di Gregorio F, Lozzi L, Cantalini C, Valentini L, Kenny JM, Delley B (2003) NO_2 and CO gas adsorption on carbon nanotubes: Experiment and theory. J Chem Phys 119:10904
71. Staii C, Johnson AT, Chen M, Gelperin A (2005) DNA-decorated carbon nanotubes for chemical sensing. Nano Lett 5:1774–1778
72. Penza M, Alvisi M, Rossi R, Serra E, Paolesse R, D'Amico A, Di Natale C (2011) Carbon nanotube films as a platform to transduce molecular recognition events in metalloporphyrins. Nanotechnology 22:125502
73. Zilberman Y, Ionescu R, Feng X, Muellen K, Haick H (2011) Nanoarray of polycyclic aromatic hydrocarbons and carbon nanotubes for accurate and predictive detection in real-world environmental humidity. ACS Nano 5:6743–6753
74. Feng XL, Marcon V, Pisula W, Hansen MR, Kirkpatrick J, Andrienko D, Kremer K, Müllen K (2009) Towards high charge-carrier mobilities by rational design of the shape and periphery of discotics. Nat Mater 8:421–426
75. Zilberman Y, Tisch U, Pisula W, Feng X, Müllen K, Haick H (2009) Sponge-like structures of hexa-peri hexabenzocoronenes derivatives enhances the sensitivity of chemiresistive carbon nanotubes to nonpolar volatile organic compounds. Langmuir 25:5411–5416
76. Kong L, Wang J, Meng F, Chen X, Jin Z, Li M, Liu J, Huang X-J (2011) Novel hybridized SWNT–PCD: synthesis and host–guest inclusion for electrical sensing recognition of persistent organic pollutants. J Mater Chem 21:11109–11115
77. Ding M, Star A (2012) Selecting fruits with carbon nanotube sensors. Angew Chem Int. https://doi.org/10.1002/anie.201203387
78. Kim W, Javey A, Vermesh O, Wang Q, Li Y, Dai H (2003) Hysteresis caused by water molecules in carbon nanotube field effect transistors. Nano Lett 3:193–198
79. Muoth M, Helbling T, Durrer L, Lee S-W, Roman C, Hierold C (2010) Hysteresis-free operation of suspended carbon nanotube transistors. Nat Nanotechnol 5:589–592
80. Leenaerts O, Partoens B, Peeters FM (2008) Adsorption of H_2O, NH_3, CO, NO_2 and NO on graphene: a first-principles study. Phys Rev B 77:125416
81. Huang B, Li Z, Liu Z, Zhou G, Hao S, Wu J, Gu B-L, Duan W (2008) Adsorption of ga molecules on graphene nanoribbons and its implication for nanoscale molecule sensor. J Phys Chem C 112:13442–13446
82. Ratinac KR, Yang W, Ringer SP, Braet F (2010) Toward ubiquitous environmental gas sensors capitalizing on the promise of graphene. Environ Sci Technol 44:1167–1176
83. Dan Y, Lu Y, Kybert NJ, Luo Z, Johnson ATC (2009) Intrinsic response of grapheme vapor sensors. Nano Lett 9:1472–1475
84. Dai J, Yuan J, Gianozzi P (2009) Gas adsorption on graphene doped with B, N, Al, and S: a theoretical study. Appl Phys Lett 95:232105
85. Robinson JT, Perkins FK, Snow ES, Wei Z, Sheehan PE (2008) Reduced graphen oxide molecular sensors. Nano Lett 8:3137–3140
86. Fowler JD, Aleen MJ, Tung VC, Yang Y, Kaner RB, Weiller BH (2009) Practical chemical sensors from chemically derived graphene. ACS Nano 3:301–306
87. Li W, Geng X, Guo Y, Rong J, Gong Y, Wu L, Zhang X, Li P, Xu J, Cheng G, Sun M, Liu L (2011) Reduced graphene oxide electrically contacted graphene sensor for highly sensitive nitric oxide detection. ACS Nano 5:6955–6961
88. Chen G, Paronyan TM, Pigos EM, Harutyunyan AR (2012) Enhanced gas sensing in pristine carbon nanotubes under continuous ultraviolet light illumination. Sci Rep 2:343. https://doi.org/10.1038/srep00343
89. Bunch JS, van der Zande AM, Verbridge SS, Frank IW, Tanenbaum DM, Parpia JM, Craighead HG, McEuen PL (2007) Electromechanical resonators from graphene sheets. Science 315:490–493
90. Sakhaee-Pour A, Ahmadian MT, Vafai A (2008) Applications of single-layered graphene sheets as mass sensors and atomistic dust detectors. Solid State Commun 145:168–172
91. Jensen K, Kim K, Zettl A (2008) An atomic-resolution nanomechanical mass sensor. Nat Nanotechnol 3:533–537

92. Jia G, Wang H, Yan L, Wang X, Pei R et al (2005) Cytotoxicity of carbon nanomaterials: single-wall nanotube, multi-wall nanotube, and fullerene. Environ Sci Technol 39:1378–1383
93. Kisin ER, Murray AR, Sargent L, Lowry D, Chirila M et al (2011) Genotoxicity of carbon nanofibers: are they potentially more or less dangerous than carbon nanotubes or asbestos? Toxicol Appl Pharmacol 252:1–10
94. Tkach AV, Shurin GV, Shurin MR, Kisin ER, Murray AR, Young S-H, Star A, Fadeel B, Kagan VE, Shvedova AA (2011) Direct effects of carbon nanotubes on dendritic cells induce immune suppression upon pulmonary exposure. ACS Nano 5:5755–5762
95. Llobet E (2013) Gas sensors using carbon nanomaterials: a review. Sens Actuat B Chem 179:32–45
96. Wang X, Tao L, Hao Y, Liu Z, Chou H, Kholmanov I, Chen S, Tan C, Jayant N, Yu Q, Akinwande D, Ruoff RS (2014) Direct delamination of graphene for high-performance plastic electronics. Small 10:694–698. https://doi.org/10.1002/smll.201301892
97. Novoselov KS, Falko VI, Colombo L, Gellert PR, Schwab MG, Kim K (2012) A roadmap for grapheme. Nature. https://doi.org/10.1038/nature11458
98. Kim KS, Zhao Y, Jang H, Lee SY, Kim JM, Kim KS, Ahn JH, Kim P, Choi JY, Hong B (2009) Large-scale pattern growth of graphene films for stretchable transparent electrodes. Nature. https://doi.org/10.1038/nature07719
99. Hoseini Z, Davoodnia A, Khojastehnezhad A, Pordel M (2020) Phosphotungstic acid supported on functionalized graphene oxide nanosheets (Go-Sic_3-Nh_3-H2pw): preparation, characterization, and first catalytic application in the synthesis of amidoalkyl naphthols. Eurasian Chem Commun 2(3):398–409. https://doi.org/10.22034/ajca.2021.259593.1228
100. Kwon SY, Ciobanu CV, Petrova V, Shenoy VB, Bare˜no J, Gambin V (2009) Growth of semiconducting graphene on palladium. Petrov Nano. https://doi.org/10.1021/nl902140j
101. Lang B (1975) A LEED study of the deposition of carbon on platinum crystal surfaces. Surf Sci. https://doi.org/10.1016/0039-6028(75)90132-6
102. Castner DG, Sexton BA, Somorja G (1978) Surf Sci 71
103. N'Diaye A, Coraux J, Plasa T, Busse C, Michel T (2008) New J Phys 10: 043033
104. Hummers WS, Offeman RE (1958) Preparation of graphitic oxide. J Am Chem Soc. https://doi.org/10.1021/ja01539a017
105. Shedin F, Geim AK, Morozov SV, Hill EW, Blake P, Katsnelson MI, Novesolov KS (2007) Detection of individual gas molecules adsorbed on grapheme. Nat Mater. https://doi.org/10.1038/nmat1967
106. Chen G, Paronyan TM, Harutyunyan AR (2012) Appl Phys Lett 101: 053119)
107. Romero HE, Joshi P, Gupta AK, Gutierrez HR, Cole MW, Tadigadapa SA, Eklund PC (2009) Adsorption of ammonia on graphene. Nanotechnology. https://doi.org/10.1088/0957-4484/20/24/245501
108. Yavari F, Chen Z, Thomas AV, Ren W, Cheng HM, Koratkar N (2011) High sensitivity gas detection using a macroscopic three-dimensional graphene foam network. Sci Rep. https://doi.org/10.1038/srep00166
109. Lu GH, Ocola LE, Chen JH (2009) Appl Phys Lett 94
110. Robinson JT, Perkins FK, Snow ES, Wei ZQ, Sheehan PE (2008) Reduced graphene oxide molecular sensors. Nano Lett. https://doi.org/10.1021/nl8013007
111. Li W, Geng X, Guo Y, Rong J, Gong Y, Wu L (2011) Reduced graphene oxide electrically contacted graphene sensor for highly sensitive nitric oxide detection. ACS Nano. https://doi.org/10.1021/nn201433r
112. Romero HE, Joshi P, Gupta AK, Gutierrez HR, Cole MW, Tadigadapa SA, Eklund PC (2009) Adsorption of ammonia on grapheme. Nanotechnology. https://doi.org/10.1088/0957-4484/20/24/245501
113. Lu G, Ocola LE, Chen J (2009) Gas detection using low-temperature reduced graphene oxide sheets. Appl Phys Lett 94(8):083111
114. Singh A, Choudhary A, Haranath D, Amish G (2012) ZnO decorated luminescent graphene as a potential gas sensor at room temperature. Carbon. https://doi.org/10.1016/j.carbon.2011.08.050
115. Qin J, Cao M, Li N, Hu C (2011) Graphene-wrapped WO_3 nanoparticles with improved performances in electrical conductivity and gas sensing properties. J Chem Mater. https://doi.org/10.1039/c1jm12692j
116. An X, Yu JC, Wang Y, Hu Y (2012) WO_3 nanorods/graphene nanocomposites for high-efficiency visible-light-driven photocatalysis and NO_2 gas sensing. J Chem Mater. https://doi.org/10.1039/c2jm16709c
117. Song H, Zhang L, He C, Qu Y, Tiana Y, Lv Y (2011) Graphene sheets decorated with SnO_2 nanoparticles: in situ synthesis and highly efficient materials for cataluminescence gas sensors. J Mater Chem. https://doi.org/10.1039/c0jm04331a
118. Mao S, Cui S, Lu G, Yu K, Wena Z, Chen J (2012) Tuning gas-sensing properties of reduced graphene oxide using tin oxide nanocrystals. J Mater Chem. https://doi.org/10.1039/c2jm30378g
119. Zhou L, Shen F, Tian X, Wang D, Zhang T, Chen W (2013) Stable Cu_2O nanocrystals grown on functionalized graphene sheets and room temperature H2S gas sensing with ultrahigh sensitivity. Nanoscale. https://doi.org/10.1039/c2nr33164k
120. De Marco M, Menzel R, Bawaked SM, Mokhtar M, Obaid AY, Basahel SN, Shaffer MSP (2017) Hybrid effects in graphene oxide/carbon nanotube-supported layered double hydroxides: enhancing the CO_2 sorption properties. Carbon 123:616–627
121. Aragaw BA (2020) Reduced graphene oxide-intercalated graphene oxide nano-hybrid for enhanced photoelectrochemical water reduction. J Nanostruct Chem 10:9–18. https://doi.org/10.1007/s40097-019-00324-x
122. Robinson MT, Tung J, Heydari M, Gleason KK (2021) Humidity-initiated gas sensors for volatile organic compounds sensing. Adv Funct Mater 31:2101310. https://doi.org/10.1002/adfm.202101310
123. Majhi SM, Mirzaei A, Navale S, Kim HW, Kim SS (2021) Boosting the sensing properties of resistive-based gas sensors by irradiation techniques: a review. Nanoscale 13:4728. https://doi.org/10.1039/D0NR08448D
124. Jingjing Y, Tsow F, Mora SJ, Tipparaju VV, Xian X (2021) Hydrogel-incorporated colorimetric sensors with high humidity tolerance for environmental gases sensing. Sens Actuat B Chem 345:130404
125. Lei G, Lou C, Liu X, Xie J, Li Z, Zheng W, Zhang J (2021) Thin films of tungsten oxide materials for advanced gas sensors. Sens Actuat B Chem 341:129996
126. Lou C, Wang K, Mei H, Xie J, Zheng W, Liu X, Zhang J (2021) ZnO nanoarrays via a thermal decomposition–deposition method for sensitive and selective NO_2 detection. Cryst Eng Comm 23:3654–3663. https://doi.org/10.1039/D1CE00410G
127. Lu Z, Ma Z, Song P et al (2021) Facile synthesis of CuO nanoribbons/rGO nanocomposites for high-performance formaldehyde gas sensor at low temperature. J Mater Sci Mater Electron 32:19297–19308. https://doi.org/10.1007/s10854-021-06449-6
128. Wetchakun K, Samerjai T, Tamaekong N, Liewhiran C, Siriwong C, Kruefu V, Wisitsoraat A, Tuantranont A, Phanichphant S (2011) Semiconducting metal oxides as sensors for environmentally hazardous gases. Sens Actuat B: Chem 160:580–591
129. Xu YS, Xie JY, Zhang YF, Tian FH, Yang C, Zheng W, Liu XH, Zhang J, Pinna N (2021) Edge-enriched WS2 nanosheets on carbon nanofibers boosts NO_2 detection at room temperature. J Hazard Mater 411:125120

130. Guo WW, Zhou QL, Zhang J, Fu M, Radacsi N, Li YX (2019) Hydrothermal synthesis of Bi-doped SnO2/rGO nanocomposites and the enhanced gas sensing performance to benzene. Sens Actuat B Chem 299:126959
131. Yin L, Wang HB, Li L, Li H, Chen DL, Zhang R (2019) Microwave-assisted preparation of hierarchical CuO@rGO nanostructures and their enhanced low-temperature H_2S-sensing performance. Appl Surf Sci 476:107–114
132. Mirmotallebi M, Irajizad A, Hosseini ZS, Jokar E (2018) Characterization of three-dimensional reduced graphene oxide/copper oxide heterostructures for hydrogen sulfide gas sensing application. J Alloys Compd 740:1024–1031
133. Bai SL, Sun X, Han N, Shu X, Pan JL, Guo HP, Liu SH, Feng YJ, Luo RX, Li DQ, Chen AF (2019) rGO modified nanoplate-assembled ZnO/CdO junction for detection of NO_2. J Hazard Mater 394:121832
134. Chao Y, Lu HB, Gao JZ, Zhang Y, Guo QM, Ding HX, Wang YT, Wei FF, Zhu GQ, Yang ZB, Wang CL (2018) Improved NO_2 sensing properties at low temperature using reduced graphene oxide nanosheet–In2O3 heterojunction nanofibers. J Alloys Compd 741:908–917
135. Yin FF, Li Y, Yue WJ, Gao S, Chen ZX (2020) Sn_3O_4/rGO heterostructure as a material for formaldehyde gas sensor with a wide detecting range and low operating temperature. Sens Actuat B Chem. 312:127954
136. Shewale PS, Yun KS (2020) Synthesis and characterization of Cu-doped ZnO/rGO nanocomposites for room-temperature H2S gas sensor. J Alloys Compd 837:155527
137. Xu YS, Zheng LL, Yang C, Liu XH, Zhang J (2020) Highly sensitive and selective electronic sensor based on Co catalyzed SnO_2 nanospheres for acetone detection. Sens. Actuat B Chem. 304:127237
138. Li ZJ, Liu YY, Guo DF, Guo JJ, Su YL (2018) Room-temperature synthesis of CuO/reduced graphene oxide nanohybrids for high-performance NO2 gas sensor. Sens Actuat B Chem 271:306–310
139. Xu YS, Zheng W, Liu XH, Zhang LQ, Zheng LL, Yang C, Pinna N, Zhang J (2020) Platinum single atoms on tin oxide ultrathin films for extremely sensitive gas detection. Mater Horiz 7:1519
140. Ganesh BS, Peramaiah K, Miriam JC, Kumar LS, Jeehyeong AK, Bernaurdshaw N (2019) Synergistic effect of sono-photocatalytic process for the degradation of organic pollutants using CuO-TiO_2/rGO. Ultrason Sonochem 50:218–223
141. Liu M, Wang ZY, Song P, Yang ZX, Wang Q (2021) Flexible MXene/rGO/CuO hybrid aerogels for high performance acetone sensing at room temperature. Sens Actuat B Chem 340:129946
142. Ma HQ, Sun X, Wang MJ, Zhang JS (2018) Regenerable CuO/gamma-Al2O3-reduced graphene oxide adsorbent with a high adsorption capacity for dibenzothiophene from model diesel oil. Ind Eng Chem Res 57:10945–10955
143. Yang ZQ, Hao XP, Chen SG, Ma ZQ, Guo ZH (2019) Long-term antibacterial stable reduced graphene oxide nanocomposites loaded with cuprous oxide nanoparticles. J Coll Interface Sci 533:13–23
144. Sharma K, Maiti K, Kim NH, Hui D, Lee JH (2018) Green synthesis of glucose-reduced graphene oxide supported Ag-Cu_2O nanocomposites for the enhanced visible-light photocatalytic activity. Compos Part B-Eng 138:35–44
145. Shahrokhian S, Rezaee S (2018) Vertically standing Cu_2O nanosheets promoted flower-like PtPd nanostructures supported on reduced graphene oxide for methanol electro-oxidation. Electrochim Acta 259:36–47
146. Zhang D, Jiang C, Wu J (2018) Layer-by-layer assembled In2O3 nanocubes/flower-like MoS2 nanofilm for room temperature formaldehyde sensing. Sens Actuat B Chem 273:176–184
147. Gong SY, Chen JY, Wu XF, Han N, Chen YF (2018) In-situ synthesis of Cu2O/reduced graphene oxide composite as effective catalyst for ozone decomposition. Catal Commun 106:25–29
148. Wei Q, Sun J, Song P, Li J, Yang ZX, Wang Q (2020) MOF-derived α-Fe_2O_3 porous spindle combined with reduced graphene oxide for improvement of TEA sensing performance. Sens Actuat B Chem 304:127306
149. Ma ZR, Song P, Yang ZX, Wang Q (2019) Trimethylamine detection of 3D rGO/mesoporous In_2O_3 nanocomposites at room temperature. Appl Surf Sci 465:625–634
150. Wang XY, Huang BY, Wu XF, Gu D, Li XG (2021) Enhanced ammonia sensing properties of rGO/WS2 heterojunction based chemiresistive sensor by marginal sulfonate decoration. Sens Actuat B 337:129776
151. Zhang J, Liu XH, Neri G, Pinna N (2016) Nanostructured materials for room-temperature gas sensors. Adv Mater 28:795–831
152. Schmidt S, Greczynski G, Goyenola C, Gueorguiev GK, Czigány ZS, Jensen J, Ivanov IG, Hultman L (2011) CFx thin solid films deposited by high power impulse magnetron sputtering: synthesis and characterization. Surf Coat Technol 206(4):646–653
153. Bakoglidis KD, Palisaitis J, dos Santos RB, Rivelino R, Persson POÅ, Gueorguiev GK, Hultman L (2018) Self-healing in carbon nitride evidenced as material inflation and superlubric behavior. ACS Appl Mater Interf 10(19):16238–16243. https://doi.org/10.1021/acsami.8b03055
154. Högberg H, Lai C-C, Broitman E, Ivanov IG, Goyenola C, Näslund L-Å, Schmidt S, Hultman L, Rosen J, Gueorguiev GK (2020) Reactive sputtering of CSx thin solid films using CS2 as precursor. Vacuum 182:109775
155. Alexeeva OK, Fateev VN (2016) Application of the magnetron sputtering for nanostructured electrocatalysts synthesis. Int J Hydrogen Energy 41(5):3373–3386
156. Sui T, Marelli D, Sun X, Fu M (2020) Multi-sensor state estimation over lossy channels using coded measurements. Automat (Oxf) 111:108561. https://doi.org/10.1016/j.automatica.2019.108561
157. Wang L, Peng Y, Xie Y, Chen B, Du Y (2021) A new iteration regularization method for dynamic load identification of stochastic structures. Mech Syst Signal Process 156:107586. https://doi.org/10.1016/j.ymssp.2020.107586
158. Gong C, Hu Y, Gao J, Wang Y, Yan L (2020) An improved delay-suppressed sliding-mode observer for sensorless vector-controlled PMSM. IEEE Trans Ind Electron 67(7):5913–5923. https://doi.org/10.1109/TIE.2019.2952824
159. Zhang T, Wu X, Shaheen SM, Rinklebe J, Bolan NS, Ali EF, Tsang DCW (2021) Effects of microorganism-mediated inoculants on humification processes and phosphorus dynamics during the aerobic composting of swine manure. J Hazard Mater 416:125738. https://doi.org/10.1016/j.jhazmat.2021.125738
160. Zhang M, Zhang L, Tian S, Zhang X, Guo J, Guan X, Xu P (2020) Effects of graphite particles/Fe_{3+} on the properties of anoxic activated sludge. Chemosp (Oxf) 253:126638. https://doi.org/10.1016/j.chemosphere.2020.126638
161. Miao Z, Xiaohe S, Xuewu O, Yongbing T (2019) Rechargeable batteries based on anion intercalation graphite cathodes. Energy Storage Mater 16:65–84. https://doi.org/10.1016/j.ensm.2018.04.023
162. Salimi M, Pirouzfar V, Kianfar E (2017) Enhanced gas transport properties in silica nanoparticle filler-polystyrene nanocomposite membranes. Coll Polym Sci 295:215–226. https://doi.org/10.1007/s00396-016-3998-0
163. Kianfar E (2018) Synthesis and characterization of AlPO4/ZSM-5 catalyst for methanol conversion to dimethyl ether. Russ J Appl Chem 91:1711–1720. https://doi.org/10.1134/S1070427218100208

164. Kianfar E (2019) Ethylene to propylene conversion over Ni-W/ZSM-5 catalyst. Russ J Appl Chem 92:1094–1101. https://doi.org/10.1134/S1070427219080068
165. Kianfar E, Salimi M, Kianfar F et al (2019) CO_2/N_2 Separation using polyvinyl chloride iso-phthalic acid/aluminium nitrate nanocomposite membrane. Macromol Res 27:83–89. https://doi.org/10.1007/s13233-019-7009-4
166. Kianfar E (2019) Ethylene to propylene over zeolite ZSM-5: improved catalyst performance by treatment with CuO. Russ J Appl Chem 92:933–939. https://doi.org/10.1134/S1070427219070085
167. Kianfar E, Shirshahi M, Kianfar F et al (2018) Simultaneous prediction of the density, viscosity and electrical conductivity of pyridinium-based hydrophobic ionic liquids using artificial neural network. SILICON 10:2617–2625. https://doi.org/10.1007/s12633-018-9798-z
168. Salimi M, Pirouzfar V, Kianfar E (2017) Novel nanocomposite membranes prepared with PVC/ABS and silica nanoparticles for C2H6/CH4 separation. Polym Sci Ser A 59:566–574. https://doi.org/10.1134/S0965545X17040071
169. Kianfar F, Kianfar E (2019) Synthesis of isophthalic acid/aluminum nitrate thin film nanocomposite membrane for hard water softening. J Inorg Organomet Polym 29:2176–2185. https://doi.org/10.1007/s10904-019-01177-1
170. Kianfar E, Azimikia R, Faghih SM (2020) Simple and strong dative attachment of α-diimine nickel (II) catalysts on supports for ethylene polymerization with controlled morphology. Catal Lett 150:2322–2330. https://doi.org/10.1007/s10562-020-03116-z
171. Kianfar E (2019) Nanozeolites: synthesized, properties, applications. J Sol Gel Sci Technol 91:415–429. https://doi.org/10.1007/s10971-019-05012-4
172. Liu H, Kianfar E (2020) Investigation the synthesis of nano-SAPO-34 catalyst prepared by different templates for MTO process. Catal Lett. https://doi.org/10.1007/s10562-020-03333-6
173. Kianfar E, Salimi M, Hajimirzaee S, Koohestani B (2018) Methanol to gasoline conversion over CuO/ZSM-5 catalyst synthesized using sonochemistry method. Int J Chem React Eng. https://doi.org/10.1515/ijcre-2018-0127
174. Kianfar E, Salimi M, Pirouzfar V, Koohestani B (2018) Synthesis of modified catalyst and stabilization of CuO/NH 4-ZSM-5 for conversion of methanol to gasoline. Int J Appl Ceram Technol 15:734–741
175. Kianfar E, Salimi M, Pirouzfar V, Koohestani B (2018) Synthesis and modification of zeolite ZSM-5 catalyst with solutions of calcium carbonate ($CaCO_3$) and sodium carbonate (Na_2CO_3) for methanol to gasoline conversion. Int J Chem React Eng 1(16):7
176. Ehsan K (2020) Comparison and assessment of Zeolite Catalysts Performance Dimethyl ether and light olefins production through methanol: a review. Rev Inorg Chem 39:157–177
177. Ehsan K, Mahmoud S (2020) A review on the production of light olefins from hydrocarbons cracking and methanol conversion: In: Taylor JC (eds) Advances in chemistry research, volume 59, Chapter: 1. Nova Science Publishers, Inc.
178. Ehsan K, Ali R (2020) Zeolite catalyst based selective for the process MTG: a review: In: Annett M (ed) Zeolites: advances in research and applications, Chapter: 8. Nova Science Publishers, Inc.
179. Ehsan K (2020) Zeolites: properties, applications, modification and selectivity: In: Annett M (ed) Zeolites: advances in research and applications, Chapter: 1. Nova Science Publishers
180. Kianfar E, Hajimirzaee S, Musavian SS, Mehr AS (2020) Zeolite-based Catalysts for Methanol to Gasoline process: A review. Microchemical J 2020:104822
181. Kianfar E, Baghernejad M, Rahimdashti Y (2015) Study synthesis of vanadium oxide nanotubes with two template hexadecylamin and hexylamine. Biol Forum 7:1671–1685
182. Ehsan kianfar. Synthesizing of vanadium oxide nanotubes using hydrothermal and ultrasonic method. Lambert Academic Publishing. 2020: 1–80. ISBN: 978–613–9–81541–8.
183. Kianfar E, Pirouzfar V, Sakhaeinia H (2017) An experimental study on absorption/stripping CO_2 using Mono-ethanol amine hollow fiber membrane contactor. J Taiwan Inst Chem Eng 80:954–962
184. Kianfar E, Viet C (2021) Polymeric membranes on base of Poly-Methyl methacrylate for air separation: a review. J Market Res 10:1437–1461
185. Snmousavian S, Faravar P, Zarei Z, Zimikia R, Monjezi MG, Kianfar E (2020) Modeling and simulation absorption of CO_2 using hollow fiber membranes (HFM) with mono-ethanol amine with computational fluid dynamics. J Environ Chem Eng 8(4):103946
186. Adewole BZ, Malomo BO, Olatunji OP, Ikobayo AO (2020) Simulation and experimental verification of electrical power output of a microcontroller based solar tracking photovoltaic module. Int J Sustain Energy Environ Res 9(1):34–45. https://doi.org/10.18488/journal.13.2020.91.34.45
187. Al-Shawi SG, Andreevna Alekhina N, Aravindhan S, Thangavelu L, Elena A, Viktorovna Kartamysheva N, Rafkatovna Zakieva R (2021) Synthesis of NiO nanoparticles and sulfur, and nitrogen co doped-graphene quantum dots/nio nanocomposites for antibacterial application. J Nanostruct 11(1):181–188
188. Khameneh Asl S, Namdar M (2019) Preparation of graphene/graphene oxide microsupercapacitor by using laser-scribed method. Chem Methodol 3(2):183–193. https://doi.org/10.22034/chemm.2018.144016.1073
189. Khosravanian A, Moslehipour A, Ashrafian H (2021) A review on bioimaging, biosensing, and drug delivery systems based on graphene quantum dots. Prog Chem Biochem Res 4(1):44–56. https://doi.org/10.22034/pcbr.2020.237134.1102
190. Davoodnia A (2011) A highly efficient and fast method for the synthesis of biscoumarins using tetrabutylammonium hexatungstate [TBA] 2 [W 6 O 19] as green and reusable heterogeneous catalyst. Bull Korean Chem Soc 32(12):4286–4290. https://doi.org/10.5012/bkcs.2011.32.12.4286
191. Alwan S, Al-Saeed M, Abid H (2021) Safety assessment and biochemical evaluation of biogenic silver nanoparticles (using bark extract of *C. zeylanicum*) in *Rattus norvegicus* rats: safety of biofabricated AgNPs (using *Cinnamomum zeylanicum* extract). Baghdad J Biochem Appl Biol Sci 2(03):138–150. https://doi.org/10.47419/bjbabs.v2i03.67
192. Nguyen DD, Moghaddam H, Pirouzfar V, Fayyazbakhsh A, Su C-H (2021) Improving the gasoline properties by blending butanol-Al_2O_3 to optimize the engine performance and reduce air pollution. Energy 218:119442
193. Fayyazbakhsh A, Pirouzfar V (2017) Comprehensive overview on diesel additives to reduce emissions, enhance fuel properties and improve engine performance. Renew Sustain Energy Rev 74:891–901
194. Khorramshokouh S, Pirouzfar V, Kazerouni Y, Fayyazbakhsh A, Abedini R (2016) Improving the properties and engine performance of diesel–methanol nanoparticle blend fuels via optimization of the emissions and engine performance. Energy Fuels 30(10):8200–8208. https://doi.org/10.1021/acs.energyfuels.6b01856
195. Fayyazbakhsh A, Pirouzfar V (2016) Investigating the influence of additives-fuel on diesel engine performance and emissions: analytical modeling and experimental validation. Fuel 171:167–177

196. Yang Z, Zhang L, Zhou Y, Wang H, Wen L, Kianfar E (2020) Investigation of effective parameters on SAPO-34 Nano catalyst the methanol-to-olefin conversion process: a review. Rev Inorg Chem 40(3):91–105. https://doi.org/10.1515/revic-2020-0003
197. Zhang X, Tang Y, Zhang F, Lee C (2016) A novel aluminum-graphite dual-ion battery. Adv Energy Mater 6(11):1502588. https://doi.org/10.1002/aenm.201502588
198. Tong X, Zhang F, Ji B, Sheng M, Tang Y (2016) Carbon-coated porous aluminum foil anode for high-rate, long-term cycling stability, and high energy density dual-ion batteries. Adv Mater (Weinh) 28(45):9979–9985. https://doi.org/10.1002/adma.201603735
199. Dong P, Zhang T, Xiang H, Xu X, Lv Y, Wang Y, Lu C (2021) Controllable synthesis of exceptionally small-sized superparamagnetic magnetite nanoparticles for ultrasensitive MR imaging and angiography. J Mater Chem B Materi Biol Med 9(4):958–968. https://doi.org/10.1039/D0TB02337J
200. Wang Z, Zhang T, Pi L, Xiang H, Dong P, Lu C, Jin T (2021) Large-scale one-pot synthesis of water-soluble and biocompatible upconversion nanoparticles for dual-modal imaging. Coll Surf B Biointerfaces 198:111480. https://doi.org/10.1016/j.colsurfb.2020.111480
201. Ni Z, Cao X, Wang X, Zhou S, Zhang C, Xu B, Ni Y (2021) Facile synthesis of copper(I) oxide nanochains and the photothermal conversion performance of its nanofluids. Coatings 11:749. https://doi.org/10.3390/coatings11070749
202. Deng X, Xu T, Huang G, Li Q, Luo L, Zhao Y, Zhu B (2021) Design and fabrication of a novel dual-frequency confocal ultrasound transducer for microvessels super-harmonic imaging. IEEE Trans Ultrason Ferroelect Freq Control 68(4):1272–1277. https://doi.org/10.1109/TUFFC.2020.3028505
203. Kianfar E, Salimi M, Koohestani B (2020) Zeolite CATALYST: a review on the production of light olefins. Lambert Academic Publishing, pp 1–116. ISBN:978-620-3-04259-7.
204. Kianfar E (2020). Investigation on catalysts of "Methanol to light Olefins". Lambert Academic Publishing, pp 1–168. ISBN: 978-620-3-19402-9.
205. Kianfar E (2020) Application of nanotechnology in enhanced recovery oil and gas importance and applications of nanotechnology, vol. 5, Chapter 3. MedDocs Publishers. pp. 16–21.
206. Kianfar E (2020) Catalytic properties of nanomaterials and factors affecting it importance amd applications of nanotechnology, Vol. 5, Chapter 4. MedDocs Publishers, pp. 22–25.
207. Kianfar E, (2020). Introducing the Application of Nanotechnology in Lithium-Ion Battery Importance & Applications of Nanotechnology, MedDocs Publishers. Vol. 4, Chapter 4, pp. 1–7.
208. Ehsan K, Mazaheri H (2020) Synthesis of nanocomposite (CAU-10-H) thin-film nanocomposite (TFN) membrane for removal of color from the water. Fine Chem Eng 1:83–91
209. Ehsan K (2020) Simultaneous prediction of the density and viscosity of the ternary system water-ethanol-ethylene glycol using support vector machine. Fine Chem Eng 22:69–74
210. Ehsan K, Mahmoud S, Behnam K (2020) Methanol to gasoline conversion over CuO/ZSM-5 catalyst synthesized and influence of water on conversion. Fine Chem Eng 1:75–82
211. Kianfar E (2020) An experimental study PVDF and PSF hollow fiber membranes for chemical absorption carbon dioxide. Fine Chem Eng 1:92–103
212. Ehsan K, Sajjad M (2020) Ionic liquids: properties, application, and synthesis. Fine Chem Eng 2:22–31
213. Faghih SM, Kianfar E (2018) Modeling of fluid bed reactor of ethylene dichloride production in Abadan Petrochemical based on three-phase hydrodynamic model. Int J Chem React Eng 16:1–14
214. Ehsan K, Mazaheri H (2020) Methanol to gasoline: a sustainable transport fuel. In: Taylor JC (ed) Advances in chemistry research, volume 66, Chapter 4. Nova Science Publishers Inc
215. Ehsan K (2020) A comparison and assessment on performance of zeolite catalyst based selective for theprocess methanol to gasoline: A Review. Advances in Chemistry Research, vol 63, Chapter 2. Nova Science Publishers, Inc, NewYork
216. Ehsan K, Saeed H, Seyed MF et al (2020) Polyvinyl chloride + nanoparticles titanium oxide membrane for separation of O_2/N_2. Advances in nanotechnology. Nova Science Publishers Inc.
217. Ehsan K (2020) Synthesis of characterization nanoparticles isophthalic acid/aluminum nitrate (CAU-10-H) using method hydrothermal. Advances in chemistry research. Nova Science Publishers, Inc.
218. Ehsan K (2020) CO_2 Capture with ionic liquids: a review. Advances in chemistry research, vol 67. Nova Science Publishers, Inc.
219. Ehsan K (2020) Enhanced light olefins production via methanol dehydration over promoted SAPO-34: Advances in Chemistry Research, vol 63, Chapter: 4. Nova Science Publishers, Inc.
220. Ehsan K (2020) Gas hydrate: applications, structure, formation, separation processes, thermodynamics. In: James CT (ed) Advances in chemistry research, vol 62, Chapter: 8. Nova Science Publishers Inc
221. Kianfar M, Kianfar F, Kianfar E (2016) The effect of nano-composites on the mechanic and morphological characteristics of NBR/PA6 blends. Am J Oil Chem Technol 4(1):29–44
222. Kianfar E (2016) The effect of nano-composites on the mechanic and morphological characteristics of NBR/PA6 blends. Am J Oil Chem Technol 4(1):27–42
223. Kianfar F (2015) Seyed reza mahdavi moghadam1 and ehsan kianfar, energy optimization of ilam gas refinery unit 100 by using HYSYS refinery software (2015). Indian J Sci Technol 8(S9):431–436
224. Kianfar E (2015) Production and identification of vanadium oxide nanotubes. Indian J Sci Technol 8(S9):455–464
225. Kianfar F (2015) Seyed reza mahdavi moghadam1 and ehsan kianfar, synthesis of spiro pyran by using silica-bonded *N*-propyldiethylenetriamine as recyclable basic catalyst, Indian. J Sci Technol 8(11):68669
226. Kianfar E (2019) Recent advances in synthesis, properties, and applications of vanadium oxide nanotube. Microchem J 145:966–978
227. Hajimirzaee S, Mehr AS, Kianfar E (2020) Modified ZSM-5 zeolite for conversion of LPG to aromatics. Polycycl Aromat Compd. https://doi.org/10.1080/10406638.2020.1833048
228. Kianfar E (2021) Investigation of the effect of crystallization temperature and time in synthesis of SAPO-34 catalyst for the production of light olefins. Pet Chem 61:527–537. https://doi.org/10.1134/S0965544121050030
229. Huang X, Zhu Y, Kianfar E (2021) Nano biosensors: properties, applications and electrochemical techniques. J Market Res 12:1649–1672. https://doi.org/10.1016/j.jmrt.2021.03.048
230. Kianfar E (2021) Protein nanoparticles in drug delivery: animal protein, plant proteins and protein cages, albumin nanoparticles. J Nanobiotechnol 19:159. https://doi.org/10.1186/s12951-021-00896-3
231. Kianfar E (2021) Magnetic nanoparticles in targeted drug delivery: a review. J Supercond Novel Magn. https://doi.org/10.1007/s10948-021-05932-9
232. Syah R, Zahar M, Kianfar E (2021) Nanoreactors: properties, applications and characterization. Int J Chem React Eng. https://doi.org/10.1515/ijcre-2021-0069
233. Kianfar E (2021) Исследование влияния температуры и времени кристаллизации при синтезе катализатора SAPO-34

для получения легких олефинов. Нефтехимия 61(3):430–442. https://doi.org/10.31857/S002824212103014X.
234. Talavari A, Ghanavati B, Azimi A, Sayyahi S (2021) PVDF/MWCNT hollow fiber mixed matrix membranes for gas absorption by Al_2O_3 nanofluid. Prog Chem Biochem Res 4(2):177–190. https://doi.org/10.22034/pcbr.2021.270178.1177
235. Ariaei S (2019) Adsorptions of diatomic gaseous molecules (H_2, N_2 and CO) on the surface of Li+@C16B8P8 fullerene-like nanostructure: computational studies. Adv J Chem Sect B 1(1):29–36
236. Molaeian M, Davood A, Mirzaei M (2020) Non-covalent interactions of *N*-(4-carboxyphenyl) phthalimide with CNTs. Adv J Chem Sect B 2(1):39–45
237. Sami P, Sani MH, Behzadnia H, Shen C (2020) Refractive index sensor for detection of N_2, He and CO_2 gases based on square resonance nanocavity in 2D photonic crystal. J Res Sci Eng Technol 8(4):74–83
238. Saida P, Dmitry G, Nafsen K, Kristina B, Georgiy A (2018) Theoretical study of graphene nanoparticles surface effects on removal of pharmaceuticals contaminants from water by neural network computational method. J Res Sci Eng Technol 6(03):15–24
239. Acharya S (2020) Preparation, electrochemical characterization and vapour sensing application of nanoporous activated carbon derived from lapsi. Prog Chem Biochem Research 3(4):350–365
240. Khameneh Asl S, Namdar M (2019) Preparation of graphene/graphene oxide microsupercapacitor by using Laser–Scribed method. Chem Methodol 3(2):183–193
241. Ozkendir OM, Gunaydin S, Mirzaei M (2019) Electronic structure study of the LiBC3 borocarbide graphene material. Adv J Chem Sect B 1(1):37–41
242. Chen H, Heidari AA, Chen H, Wang M, Pan Z, Gandomi AH (2020) Multi-population differential evolution-assisted Harris hawks optimization: framework and case studies. Fut Gen Comput Syst 111:175–198. https://doi.org/10.1016/j.future.2020.04.008
243. Wang M, Chen H (2020) Chaotic multi-swarm whale optimizer boosted support vector machine for medical diagnosis. Appl Soft Comput 88:105946. https://doi.org/10.1016/j.asoc.2019.105946
244. Xu Y, Chen H, Luo J, Zhang Q, Jiao S, Zhang X (2019) Enhanced Moth-flame optimizer with mutation strategy for global optimization. Inform Sci 492:181–203. https://doi.org/10.1016/j.ins.2019.04.022
245. Zhao X, Zhang X, Cai Z, Tian X, Wang X, Huang Y, Chen H, Hu L (2019) Chaos enhanced grey wolf optimization wrapped ELM for diagnosis of paraquat-poisoned patients. Comput Biol Chem 78:481–490. https://doi.org/10.1016/j.compbiolchem.2018.11.017
246. Li C, Hou L, Sharma B, Li H, Chen C, Li Y, Zhao X, Huang H, Cai Z, Chen H (2018) Developing a new intelligent system for the diagnosis of tuberculous pleural effusion. Comput Methods Prog Biomed 153:211–225. https://doi.org/10.1016/j.cmpb.2017.10.022
247. Wang M, Chen H, Yang B, Zhao X, Hu L, Cai Z, Huang H, Tong C (2017) Toward an optimal kernel extreme learning machine using a chaotic moth-flame optimization strategy with applications in medical diagnoses. Neurocomputing 267:69–84. https://doi.org/10.1016/j.neucom.2017.04.060
248. Xia J, Chen H, Li Q, Zhou M, Chen L, Cai Z, Fang Y, Zhou H (2017) Ultrasound-based differentiation of malignant and benign thyroid nodules: an extreme learning machine approach. Comput Methods Prog Biomed 147:37–49. https://doi.org/10.1016/j.cmpb.2017.06.005
249. Chen H-L, Wang G, Ma C, Cai Z-N, Liu W-B, Wang S-J (2016) An efficient hybrid kernel extreme learning machine approach for early diagnosis of Parkinson's disease. Neurocomputing 184:131–144. https://doi.org/10.1016/j.neucom.2015.07.138
250. Shen L, Chen H, Yu Z, Kang W, Zhang B, Li H, Yang B, Liu D (2016) Evolving support vector machines using fruit fly optimization for medical data classification. Knowl Based Syst 96:61–75. https://doi.org/10.1016/j.knosys.2016.01.002
251. Lufeng H, Hong G, Ma J, Wang X, Chen H (2015) An efficient machine learning approach for diagnosis of paraquat-poisoned patients. Comput Biol Med 59:116–124. https://doi.org/10.1016/j.compbiomed.2015.02.003
252. Xu X, Chen H-L (2014) Adaptive computational chemotaxis based on field in bacterial foraging optimization. Soft Comput 18(4):797–807. https://doi.org/10.1007/s00500-013-1089-4
253. Zhang Y, Liu R, Wang X, Chen H, Li C (2020) Boosted binary Harris hawks optimizer and feature selection. Eng Comput. https://doi.org/10.1007/s00366-020-01028-5
254. Zhang Y et al (2020) Towards augmented kernel extreme learning models for bankruptcy prediction: algorithmic behavior and comprehensive analysis. Neurocomputing. https://doi.org/10.1016/j.neucom.2020.10.038
255. Zhao D et al (2020) Chaotic random spare ant colony optimization for multi-threshold image segmentation of 2D Kapur entropy. Knowl Based Syst. https://doi.org/10.1016/j.knosys.2020.106510
256. Tu J et al (2020) Evolutionary biogeography-based Whale optimization methods with communication structure: towards measuring the balance. Based Syst Knowl. https://doi.org/10.1016/j.knosys.2020.106642
257. Shan W et al (2020) Double adaptive weights for stabilization of moth flame optimizer: Balance analysis, engineering cases, and medical diagnosis. Knowl Based Syst. https://doi.org/10.1016/j.knosys.2020.106728
258. Yu C et al (2021) SGOA: annealing-behaved grasshopper optimizer for global tasks. Eng Comput. https://doi.org/10.1007/s00366-020-01234-1
259. Hu J et al (2021) Orthogonal learning covariance matrix for defects of grey wolf optimizer: Insights, balance, diversity, and feature selection. Knowl Based Syst 213:106684. https://doi.org/10.1016/j.knosys.2020.106684
260. Zhao X, Li D, Yang B, Ma C, Zhu Y, Chen H (2014) Feature selection based on improved ant colony optimization for online detection of foreign fiber in cotton. Appl Soft Comput 24:585–596. https://doi.org/10.1016/j.asoc.2014.07.024
261. Yu H, Li W, Chen C, Liang J, Gui W, Wang M, Chen H (2020) Dynamic Gaussian bare-bones fruit fly optimizers with abandonment mechanism: method and analysis. Comput Eng. https://doi.org/10.1007/s00366-020-01174-w
262. Goyenola C, Gueorguiev GK, Stafström S, Hultman L (2011) Fullerene-like CSx: a first-principles study of synthetic growth. Chem Phys Lett 506(1–3):86–91
263. Isola LA, Chen TC, Elveny M, Alkaim AF, Thangavelu L, Kianfar E (2021) Application of micro and porous materials as nano-reactors. Rev Inorg Chem. https://doi.org/10.1515/revic-2021-0007